Post-translational polymodification of the C-terminal tail of *TUBB1* regulates motor protein processivity in platelet production and function

Abdullah O. Khan[1,✉], Alexandre Slater[1], Annabel Maclachlan[1], Phillip L.R. Nicolson[1], Jeremy A. Pike[2], Jack Yule[2], Steven G. Thomas[1,2], and Neil V. Morgan[1✉]

[1]Institute of Cardiovascular Science, College of Medical and Dental Sciences, University of Birmingham, Edgbaston, B15 2TT
[2]Centre of Membrane and Protein and Receptors (COMPARE), University of Birmingham and University of Nottingham, Midlands, UK

Microtubules are ubiquitously expressed cytoskeletal structures responsible for a host of cellular processes from division to cargo transport. In specialised cells, the expression of specific isoforms of tubulin and their subsequent post-translational modifications are thought to drive and co-ordinate unique morphologies and behaviours. The mechanisms by which β-1 tubulin (encoded by *TUBB1*), the platelet and megakaryocytic specific β-tubulin isoform required for platelet production and function, drives these processes remains poorly understood. We investigate the effects of two key tubulin post-translational polymodifications (polyglutamylation and polyglycylation) on the glutamate rich C-terminus of β-1 tubulin using a cohort of thrombocytopenic patients, human induced pluripotent stem cell (iPSC) derived megakaryocytes, and healthy human donor platelets. We find that while megakaryocytes (MKs) are positive for both polymodifications, polyglycylation is substantially reduced on platelets. On platelet activation, the marginal band becomes heavily polyglutamylated, which drives the mobilisation of motor proteins, including axonemal dynein, to achieve the shape change required for the haemostatic role of platelets. Finally, we show that a number of modifying enzymes (Tubulin Tyrosine Like Ligases (TTLLs) and Cytosolic Carboxypeptidases (CCPs)) are up-regulated through MK maturation. In platelets, a single polyglutamylase (TTLL7) is expressed to mediate the polyglutamylation of the marginal band required for shape change on activation. Finally, we report a novel disease causing gene in multiple families (TTLL10) resulting in bleeding despite normal platelet production and function. This work highlights the importance of a complex regulatory mechanism driven by both cell specific tubulin isoform expression and differential post-translational modification to drive specialist function, the loss of which results in disease states.

tubulin code | TUBB1 | megakaryocyte | platelet | motor protein | thrombocytopenia

Correspondence: *a.khan.4@bham.ac.uk, N.V.Morgan@bham.ac.uk, S.Thomas @bham.ac.uk*

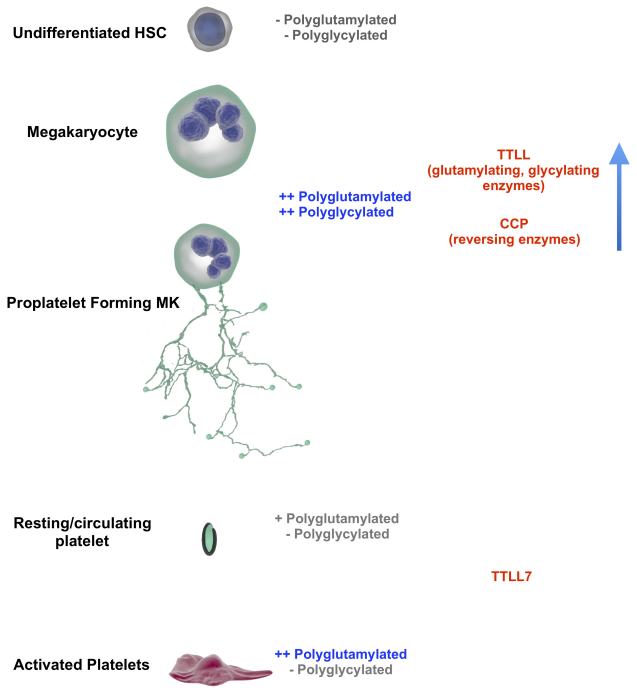

Fig. 1. Graphical Abstract In this work we report a system of reversible polymodification (polyglutamylation and polyglycylation) of the MK and platelet specific β-1 tubulin isoform required for platelet production and function. These polymodifications are driven by an up-regulation of key Tubulin Tyrosine Like Ligases (TTLLs) which mediate the addition of single glutamate or glycine residues (initiases which trigger monogluytamylation or monoglycylation), and elongases which extend a glutamate or glycine tail (polyglutamylation and polyglycylation respectively). These processes are reversed by Cytosolic Carboxypeptidase (CCP) enzymes). MKs express a range of TTLLs and CCPs, while platelets only express a single polyglutamylase, TTLL7.

Introduction

Microtubules are large, cytoskeletal filaments vital to a host of critical functions including cell division, signalling, cargo transport, motility, and function(1–3). Despite their ubiquitous expression and high structural conservation, microtubules are also critical to achieving unique morphologies and functions in specialist cell types like ciliated cells, spermatozoa, and neurons(4, 5). The question of how filaments expressed in every cell in the body can facilitate complex and highly unique behaviours like neurotransmitter release and retinal organisation has been addressed by the 'tubulin code'. This is a paradigm which accounts for the specialisation of microtubules and their organisation by describing a mechanism in which particular cells express lineage restricted isoforms of tubulin, each of which is then subject to a series

of post-translational modifications which alter the mechanical properties of microtubules, and their capacity to recruit accessory proteins (e.g. motors)(1–3, 5).

A host of tubulin post-translational modifications (PTMs) have been reported in a range of cell types, including (but not limited to) tyrosination, acetylation, glutamylation, glycylation, and phosphorylation. In recent years links between the loss of specific tubulin PTMs, either through the aberrant expression of tubulin isoforms or the loss of effecting or reversing enzymes, has emerged (5). The loss of post-translationally modified tubulin has been reported to impact motile and non-motile ciliary function (including respiratory cilia, retinal cells), spermatogenesis, muscular disorders, and neurological development and function(1, 5–11). Of the many cell systems in which careful regulation of tubulin modification is required for healthy function, the role of the tubulin code in the generation of blood platelets from their progenitors, megakaryocytes (MKs) remains relatively poorly understood.

Platelets are the smallest component of peripheral blood, and circulate as anucleate cells with an archetypal discoid shape maintained by a microtubule marginal band(12, 13). The activation of platelets involves a tightly regulated rearrangement of the cytoskeleton which results in a series of shape changes(13–15). Antagonistic motor proteins maintain the resting state of the marginal band, and during platelet activation a motor protein dependent mechanism results in sliding which extends the marginal band and causes the transition to a spherical shape (13). This change can either be transient and reversible or, in the presence of a sufficiently strong stimulus, become irreversible through actomyosin contraction and the subsequent concentration of granules to the centre of the platelets(14). The disc-to-sphere transition is a critical part of platelet activation, which also involves the secretion of granules as a terminal step in platelet activation.

Conversely megakaryocytes are the largest and rarest haematopoeitic cell of the bone marrow. These cells are characteristically large, polyploid cells with unique morphological structures (e.g. the invaginated membrane system) required to facilitate the production of thousands of blood platelets and package them with the required pro-thrombotic factors(16). Extensive cytoskeletal remodelling is critical to the maturation of MKs and the maintenance of key structures like the IMS, as well as to the production of platelets themselves(15, 16). MKs form long, beaded extensions into the lumen of bone marrow sinusoids - these proplatelet extensions then experience fission under the flow of sinusoidal blood vessels which results in the release of barbell shaped pre-platelets and platelets into the blood stream(16).

Both MKs and platelets express a lineage restricted isoform of β-tubulin encoded by the gene *TUBB1*(17). In humans, *TUBB1* mutations have been shown to result in impaired platelet production, with a resulting macrothrombocytopenia. An early report of a *TUBB1* mutation resulting in a familial congenital macrothrombocytopia by Kunisima *et al.* described low platelet counts (40-60 x 10^9/L) in a 7 year old patient initially diagnosed with idiopathic thrombocytopenia purpurra(18). This novel p.R318W mutation resulted in abnormally large platelets, however platelet aggregation, megakaryocyte number and function appeared normal. The same group followed up with a separate report in 2014 of a p.F260S mutation with a similar phenotype (19). More recently, a C-terminal truncation of β-tubulin 1 has been shown to cause a macrothrombocytopenia, suggesting that C-terminal modifications may be drivers of protein function and causative of the disease phenotype observed (20).

While the loss of *TUBB1* is known to result in macrothrombocytopenia, the mechanisms by which this isoform of tubulin effects the dramatically different cytoskeletal behaviours of platelets and MKs remains poorly understood. In the context of the tubulin code, MKs and platelets present a particularly interesting model. Both cells express a specific *TUBB1* isoform, but undergo markedly different cytoskeletal changes. To date, acetylation and tyrosination have been the PTMs primarily reported in MKs and platelets, however neither modification is exclusive to the C-terminal tail of *TUBB1* implicated by Fiore *et al.* in their report of thrombocytopenic patients with a C-terminal truncation who phenocopy patients who lose the protein completely (13, 21). We therefore hypothesise that PTMs specific to *TUBB1* are required for the complex morphological rearrangements required for both MK and platelet function.

The C-terminal tail of *TUBB1* is particularly rich in glutamate residues which are often targeted for two key post-translational modifications implicated in human disease. Polyglutamylation and glycylation are PTMs which target glutamate residues on both tubulin subunits (α and β) and result in the addition of glutamate or glycine residues respectively(1, 2, 22). Interestingly polyglutamylation has been observed in microtubules in centrioles, axenomes, neuronal outgrowths, and mitotic spindles(1, 2).

Thus far polyglycylation has primarily been observed in axenomes, suggesting a role for polyglycylation and polyglutamylation in regulating ciliary function - with important consequences for ciliopathies(1). As these polymodifications target the same substrate - namely glutamate residues in tubulin tails, there has been a level of competition observed between these PTMs. For example, glutamylation is evident on β-tubulin in post-natal development, but is found on α-tubulin in younger neurons(23). There is some debate as to whether these polymodifications negatively regulate one another(24, 25).

Ciliopathies result in a range of disorders which stem from aberrant functions in both motile cilia and flagella, but also primary cilia(7). The polyglutamaylation of C-terminal tails has been shown to be an important regulator of ciliary beating(5), with mutations in the glutamylases and deglutamylases regulating this polymodification causing male infertility through aberrant spermatogenesis and poor sperm motility(11, 26, 27). Other motile cilia include airway cilia , whose function is impaired on the loss of the polyglutamylase TTLL1 in mice(9). Beyond ciliopathies, glutamylation has significant roles in neuronal development and function. Current research suggests a role for polyglutamylation in ax-

onal transport (due to the effects of this PTM on motor protein processivity) and synaptic function(28, 29).

To date polyglycylation has not been reported in MKs or platelets. Recently Van Dijke *et al.* report on the polyglutamylation of *TUBB1* in a CHO cell line engineered to express *TUBB1* downstream of the integrin $\alpha_{2b}\beta_3$, and platelets spread on fibrinogen(30). However, to effectively study and interpret the effects of post-translationally modified tubulin residues a model is required which recapitulates the complex network of regulatory enzymes effecting and reversing PTMs. This is particularly important in light of potential evolutionary divergences in the function of TTLL enzymes implicated by Rogowski *et al.*(25).

To interrogate the polymodification of the C-terminal tail of *TUBB1* as a driver of both platelet formation and function, we report on two unrelated families with variants in the C-terminal region of *TUBB1* gene, resulting in a macrothrombocytopenia and bleeding. Existing cell lines poorly emulate the expression profiles and platelet producing capacity of MKs, and so to develop a representative model of we adapt a directed differentiation protocol to generate a large population of proplatelet forming MKs from induced pluripotent stem cells (iPSCs) and apply these cells to report on the extensive polyglycylation and polyglutamylation of proplatelet forming MKs. We demonstrate that these polymodifications are removed in resting platelets, but that upon activation, platelets undergo a hyperglutamylation of the marginal band to undergo spreading.

We go on to show that on platelet activation, kinesin and dynein poorly co-localise with polyglutamylated residues, supporting previous work which suggests that hyperglutamylation impacts motor protein processivity. We therefore reason that polyglutamylation is the mechanism by which platelet marginal bands are destabilised on activation. The role of polyglycylation in platelet activity remains unclear, however we report on patient variants in 3 unrelated families which result in a loss-of-function of the polyglycylase *TTLL10*, suggesting a role for this gene, previously thought to be non-functional in humans, in thrombus stability.

Finally, we perform an RT-PCR panel of the 13 known mammalian tubulin tyrosin like ligases (TTLLs) and 6 Cytosolic Carboxypeptidases (CCPs) and report an increase in the expression of specific TTLLs and CCPs in maturing and proplatelet forming MKs.

Our *in vitro* work identifies a mechanism by which maturing MKs are extensively polymodified to generate the unique dynein motility required for microtubule sliding, and hence proplatelet production, before a reversal of these polymodifications allows for resting, discoid platelets in circulation. We show that polyglutamylation is required for platelet activation, and likely works to increase motor protein processivity to generate the force required for the dynamic shape change observed in activated platelets and thrombus formation. We link the loss of these polymodifications to the macrothrombocytopenia evidence in patients with defective *TUBB1* expression, and report on a novel player in bleeding disorders, the polyglycylase TTLL10.

Results

A. Identification and initial characterisation of *TUBB1* variants in patients with inherited thrombocytopenia and platelet dysfunction. Two C-terminal *TUBB1* variants were identified from the GAPP cohort, each of which belong to unrelated families presenting with macrothrombocytopenia (Figure 2). Family A patients were found to be heterozygous for a C to T missense variant resulting in an arginine to tryptophan amino acid substitution (c.C1075T, p.R359W) in *TUBB1*. Individuals in this family also carry a *GFI1B* variant (p.Cys168Phe), however only individuals A:1 and A:3, both of whom carry both mutations, present with a macrothrombocytopenia (107 and 85 x 10^9/L respectively). Individual A:2, who has the *GFI1B* mutation but does not carry the *TUBB1* variant and presents with a normal platelet count (221 x 10^9/L). Interestingly, individuals A:1 and A:3 also present with significantly higher immature platelet fractions (IPFs) and mean platelet volumes (MPVs) than their *TUBB1* WT relative (53.5% and 55.1% compared to 25.5%, MPV for A:1 and A:3 too large for measurement). This variation in count and phenotype suggest that *TUBB1* is causative of the macrothrombocytopenia observed.

Family/patient B was an elderly gentleman (now deceased) with a G insertion and subsequent frameshift truncation of the protein 19 amino acids from the site of insertion (c.1080insG, p.L:361Afs*19). This patient had a severe macrothrombocytopenia with a count of 11 x 10^9/L and MPV of 13.4 (Figure 2 B). At the time of study, IPF measurement was unavailable.

Both *TUBB1* variants are positioned in the C-terminal region of the $\beta-1$ isoform encoded by *TUBB1* as indicated in figures 2 C and D. This region is positioned away from the dimer:dimer interface, and the C-terminal tail is an established site for post-translational modification (PTM) (1). Both affected nucleotides are highly conserved in mammals (Figure 2 E). We predicted that the R359W missense substitution is likely to alter the folding of the C-terminal tail, potentially affecting PTM or interactions with critical MAPs (Figure 2 C,D). Similarly the G insertion and subsequent frameshift are likely to truncate the C-terminal region.

Patient platelet function was investigated using flow cytometry due to the reduced platelet count observed. Interestingly, patient B shows a significant reduction in surface P-selectin and fibrinogen uptake in response to all agonists (Figure S1). Family A showed no change in the levels of surface receptor expression, but showed a weak P-selectin and fibrinogen response when activated with a low dose ADP, CRP, and PAR-1, suggesting a mild secretion defect (Figure S1 C,D).

Patients with C-terminal variants in this study and others previously reported by Fiore *et al.* phenocopy individuals with a complete loss of the β-1 tubulin (18–20), suggesting that the C-terminal tail is likely critical to the function of *TUBB1* in the myriad complex roles of microtubules in both MKs and platelets. As this C-terminal tail is rich in glutamate residues which are often targeted for polymodification, we began to investigate the role of polyglutamylation and polyglycylation in human stem cell derived megakaryocytes and platelets.

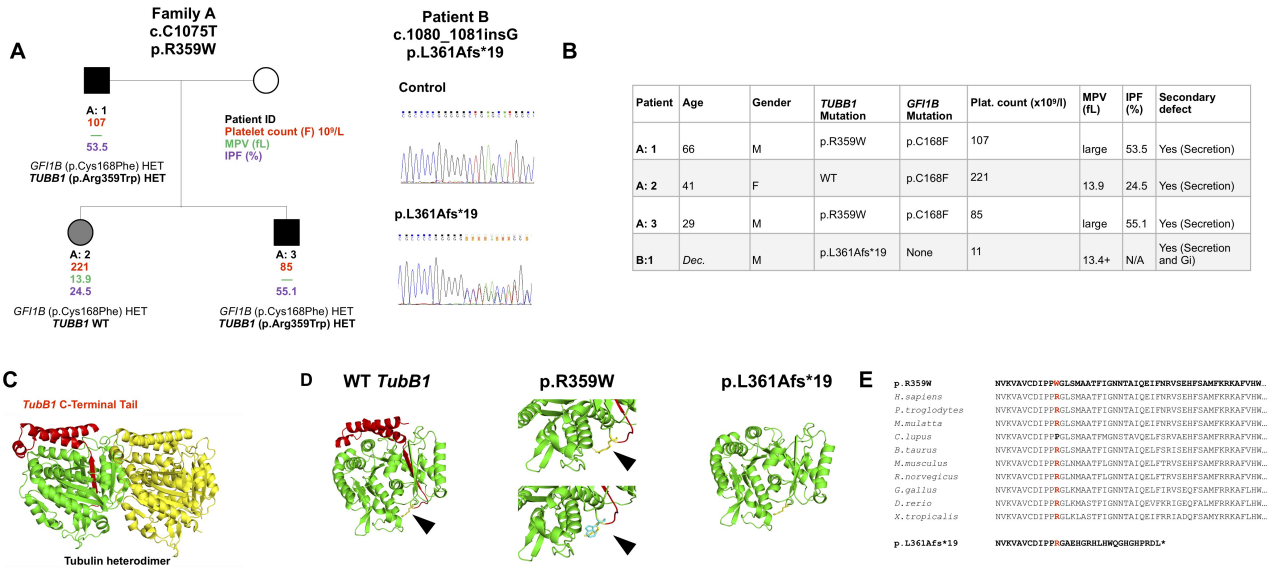

Patient	Age	Gender	*TUBB1* Mutation	*GFI1B* Mutation	Plat. count (x10⁹/l)	MPV (fL)	IPF (%)	Secondary defect
A: 1	66	M	p.R359W	p.C168F	107	large	53.5	Yes (Secretion)
A: 2	41	F	WT	p.C168F	221	13.9	24.5	Yes (Secretion)
A: 3	29	M	p.R359W	p.C168F	85	large	55.1	Yes (Secretion)
B:1	*Dec.*	M	p.L361Afs*19	None	11	13.4+	N/A	Yes (Secretion and Gi)

Fig. 2. Candidate *TUBB1* mutations and their hypothesised effect on the C-terminus of β-tubulin. (A,B) Two unrelated families were identified as carrying mutations in the *TUBB1* gene within 6 base pairs of one another. The first, family A, is comprised of 3 individuals, two of whom carry an Arginine to Tryptophan (p.R359W) coding mutation. Interestingly, all 3 individuals in family A harbour a *GFI1B* mutation. However, the individuals with the reported *TUBB1* mutation (A:1 and A:3) present with a macrothrombocytopenia and high IPF, while the patient without the R359W *TUBB1* mutation presented with a normal platelet count. The second family is comprised of a single individual, recently deceased, with a frameshift mutation 6 base pairs from the missense reported in family A. In this individual's case, the insertion of a guanine nucleotide results in a frameshift with a premature stop codon 19 amino acids from the leucine to alanine change. (C) The C-terminal tail is downstream of both mutations in these families, and projects away from the dimer/dimer interface. (D) Based on homology modelling of *TUBB1*, we predict that the missense mutation reported in family A is likely to affect the fold of the C-terminal tail, while the frameshift causes a truncation of this region. (E) The arginine residue mutated in family A is highly conserved across species, as are sequences adjacent to the frameshift in patient B.

B. iPSC-derived proplatelet forming MKs are both polyglycylated and polyglutamylated. Polyglutamylation has very recently been reported in a modified CHO cell line and human platelets, however no evidence of this PTM has been reported in human MKs. A species dependent variation in the expression of modifying enzymes has been reported and discussed, therefore a human model is required to investigate the role of this polymodification in platelet production (25, 30, 31). To date, polyglycylation has not been reported in either platelets or megakaryocytes, however both modifications target the same glutamate residue, suggesting a potentially competitive mechanism by which these PTMs are applied to β-1 tubulin.

To investigate polymodification in human megakaryocytes, we adapted a directed differentiation protocol previously reported by Feng *et al.* to generate large populations of mature, proplatelet forming cells (Supplementary Figure S2). Cells were differentiated and stained for CD42b as a marker for mature, and hence *TUBB1* expressing, MKs and both polyglutamylated and polyglycylated tubulin. CD42b positive cells, including proplatelet forming cells, were also found to be positive for both polyglutamylated tubulin and polyglycylated tubulin (Figure 3 A,B), while neighbouring cells in the sample negative for CD42b did not demonstrate these polymodifications (Figure 3 C). Across multiple differentiations we consistently yielded a purity of approximately 50-60% CD42b positive cells, which on analysis are positive for both polyglutamylated and polyglycylated tubulin. Finally, all proplatelet cells observed across replicates were positive for both polyglutamylated and polyglycylated tubulin.

C. Platelet activation results in the polyglutamylation of the marginal band. MKs and platelets both achieve markedly different morphologies and functions despite the expression of *TUBB1* in both cell types. As such we hypotheized that the *TUBB1* polymodifications evident in MKs might be differently regulated between resting and activated platelets. We therefore compared immunofluorescence staining of polyglutamylated and polyglycylated tubulin between resting platelets and cells spread on fibrinogen and collagen. We found that resting platelets demonstrate a diffuse distribution of polyglutamylated tubulin which partially co-localises with the β-tubulin marginal band. Interestingly however, we see a marked increase in the polyglutamylation of the marginal band on platelet activation and spreading on fibrinogen (**** $p < 0.0001$, *** p 0.003) (Figure 4 A). Polyglycylated tubulin however, is observed as low-level, punctate staining throughout both resting and activated cells (Figure 4 B).

Western blotting of resting platelets and cells activated through exposure to collagen related peptide (CRP) over time does not show an increase in the total amount of polyglutamylated tubulin in the sample (Figure 4 C). Interestingly, analysis of the co-localisation between β-tubulin and polymodified residues shows a significant increase in co-localisation between polyglutamylated tubulin and the marginal band in both fibrinogen and collagen spread cells. No significant change in co-localisation is observed for polyglycylated residues (Figure 4 D).

To investigate the distribution of both polyglutamylated and polyglycylated tubulin in the context of thrombi, platelets

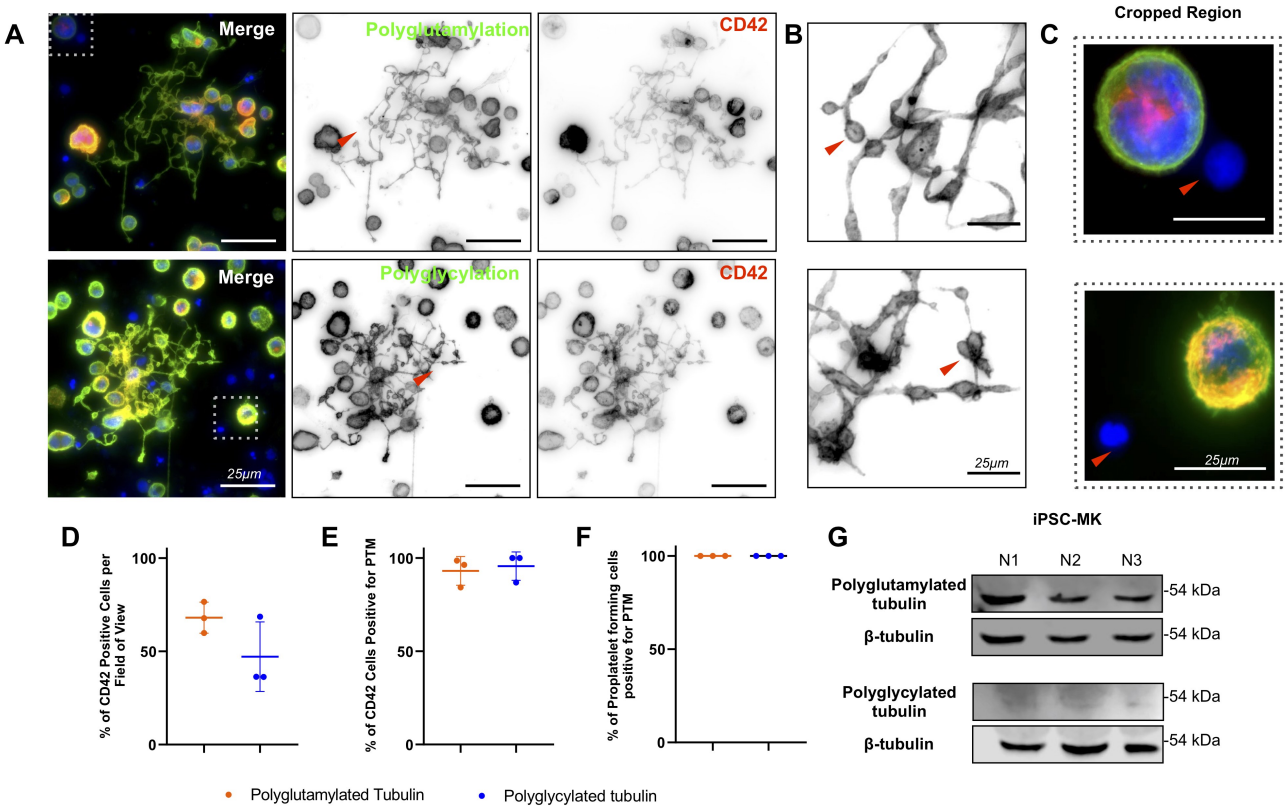

Fig. 3. Mature, proplatelet forming iPSC-MKs are both polyglutamylated and polyglcylated. (A) iPSC-MKs co-stained for CD42 and polyglycylated and polyglutamylated tubulin show that these cells are positive for both polymodifications. (B) Both polyglutamylated and polyglycylated tubulin are evident in proplatelet extensions, including nascent platelet swellings on the proplatelet shaft (indicated by red arrows). (C) Neighbouring CD42b$^-$ cells are also negative for both polymodifications, suggesting that only mature, and hence *TUBB1* expressing MKs within the sample are polymodified. (D, E) Approximately 50-60% of cells in multiple differentiations are positive for CD42b, and these cells are 100% double positive for polymodification and CD42b. (F) All proplatelet extensions observed are positive for polymodification. (G) Polyglutamylation is evident by western blotting in mature iPSC-MKs, however poor labelling by the polyglycylated antibody does not allow us to quantify total levels of each of these polymodifications.

were activated *in vitro* using CRP and subsequently fixed and mounted on to Poly-L-Lysine coated coverslips. These cells were then stained for both β-tubulin and polyglutamylated or polyglycylated tubulin respectively (Figure 4 F,G). Interestingly, polyglutamylated tubulin is evident throughout the aggregate on the marginal band of platelets, while polyglycylated tubulin is diffusely distributed (Figure 4 F,G).

Acetylation and tyrosination have been previously reported in platelets, however their role in maintaining the marginal band and/or driving morphological change on platelet activation remains unclear(13). To determine whether the polyglutamylation of the marginal band we observe thus far co-incides with these PTMs, we performed a time course of spreading on fibrinogen to determine whether there is an equivalent increase in either acetylation or tyrosination of the marginal band. Interestingly, we find no marked acetylation or tyrosination of this structure over the time course, while a notable polyglutamylation of the marginal band is evident from the earliest time point (10 minutes spreading on fibrinogen) (Figure 4 H, I).

D. Platelet and MK polymodifications regulate motor protein processivity to drive both proplatelet formation and platelet shape change on activation. Thus far we have observed a markedly different distribution of polyglutamylated and polyglycylated residues in both human iPSC-derived MKs and human donor peripheral blood platelets. Polyglutamylation has been reported as a means by which motor protein processivity is regulated, and like in neuronal cells, MK proplatelet formation is known to be driven by a mechanism of dynein mediated proplatelet sliding (32). Similarly, the antagonistic movement of dynein and kinesin are known to maintain the marginal band in resting platelets(13).

We hypothesised that polyglutamylation in both MKs and platelets increases motor protein processivity. Therefore the polyglycylation evident in MKs (but notably absent in platelets) is likely a mechanism of regulating motor protein motility to prevent excessive polyglutamylation and control the microtubule sliding required for platelet production. Interestingly, the polyglutamylation and polyglycylation of proplatelet extensions is analogous to the polymodifications observed in ciliated cells, suggesting a potential role for axonemal dyneins in facilitating these unique cellular processes.

To test this hypothesis, we first performed a time course of platelet spreading on fibrinogen and measured co-localisation between polyglutamylated tubulin and axonemal dynein

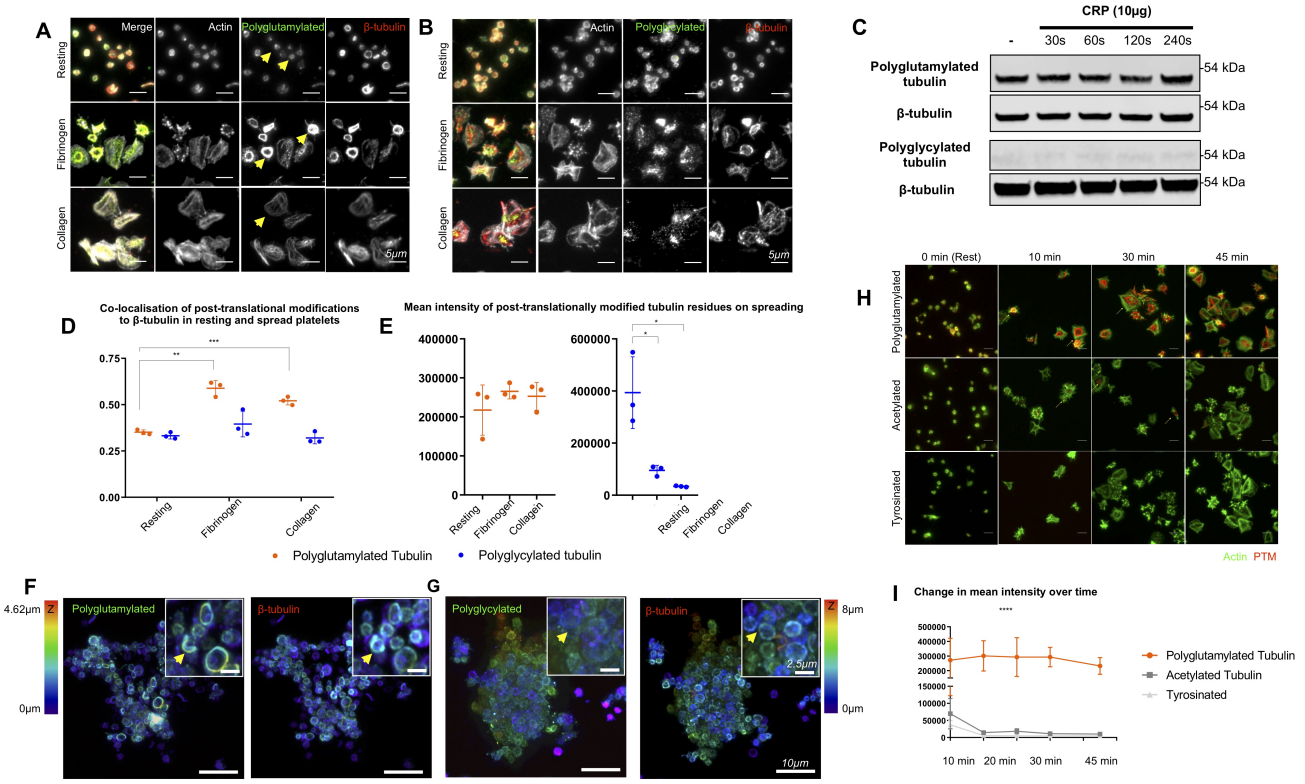

Fig. 4. Platelet activation results in polyglutamylation of the marginal band (A) Resting platelets show a diffuse distribution of polyglutamylated tubulin which partially co-localises with the marginal band (yellow arrows), however, on spreading on fibrinogen, a marked increase in the polyglutamylation of the marginal band is observed (yellow arrows). (B) Polyglycylated tubulin is similarly diffuse in resting platelets, however spreading does not show notable changes in this polymodification. (C) Western blotting shows poor detection of polyglycylated tubulin as previously observed in MK lysates, however probing for polyglutamylated tubulin across samples activated with CRP does not show a particular change in the abundance of polyglutamylated tubulin. (D) A measurement of co-localisation between polyglutamylated tubulin and β-tubulin in resting and spread platelets shows a significant increase in the co-localisation of these modified tubulin residues on platelet activation and spreading. This change localisation is not observed between polyglycylated residues and β-tubulin. (E) Measurements of fluorescence mean intensity in polyglutamylated and polyglycylated tubulin shows a change in polyglutamylated tubulin consistent with western blotting, and a decrease in polyglycylated tubulin suggesting that platelets are not actively polyglycylated as they are activated. (F) Platelets activated *in vitro* using CRP were co-stained for β-tubulin and polyglutamylated residues and imaged in 3D using AiryScan confocal (stacks colourized in Z as indicated by the colour chart in this figure). In these micro-thrombi, extensive polyglutamylation of the marginal band is evident. (G) Similar samples stained for polyglycylated tubulin show a diffuse distribution of these residues throughout the cell. (H) A time course was performed to compare polyglutamylated tubulin with two other previously reported PTMs in platelets (acetylation and tyrosination). No significant acetylation or tyrosination of the marginal band is evident over a 45 minute time course, however polyglutamylation of the marginal band is evident throughout the time course. (I) The mean fluorescence intensity of polyglutamylated tubulin is markedly higher than either acetylated or tyrosinated tubulin. ($n = 3$, *S.D.*, Two-Way ANOVA with multiple comparisons. *10 μm scale bar.*)

(DNAL1 - axonemal light chain 1). We observe a sharp loss of co-localisation between axonemal dynein and polyglutamylated residues upon platelet spreading (Figure 5 A,B). Interestingly, axonemal dynein is also localised towards the leading edge of platelets when spread on fibrinogen (Figure 5A). This data suggests that the increased polyglutamylation of the marginal band observed on platelet spreading drives an outward movement of axonemal dynein. To confirm the role of axonemal dynein specifically in this process, we also stained spreading platelets for cytoplasmic dynein and observe a central distribution, suggesting an alternative role for cytoplasmic dynein in platelets (Figure S3).

To confirm that the loss of colocalisation observed was specific to polyglutamylated residues, we co-stained resting and spread platelets (fibrinogen and collagen) for both polyglutamylated and polyglycylated tubulin and compare their co-localisation with dynein and kinesin-1, a motor protein recently reported to be important in platelet secretion (33). We found that while in both fibrinogen and collagen spread platelets a leading edge distribution of axonemal dynein is evident (Figure 5) which poorly co-localises with polyglutamylated tubulin, there is no particular spatial relationship between polygylcylated tubulin and axonemal dynein (Figure 5 C,D,E). A significant decrease in co-localisation is observed in both the fibrinogen and collagen spread cells (Figure 5 E, H).

Interestingly, kinesin-1 is evident throughout the spread platelet, and while there is a significant decrease in the co-localisation of this motor with polyglutamylated tubulin, there is no change in co-localisation between the polyglycylated residues and kinesin-1 (Figure 5 F,G,H). This data suggests that polyglutamylated tubulin accelerates motor protein motility as previously described *in vitro* assays, while polyglycylation potentially acts as a 'braking' mechanism.

In proplatelet extensions axonemal dynein and kinesin-1 are both evident along the length of the proplatelet shaft (Figure 5 I,J). A mechanism of dynein mediated sliding has been reported as the driver of proplatelet elongation, however the original work cites cytoplasmic dynein as the mediator of this effect(32). Evidence of axonemal dynein in both the platelet

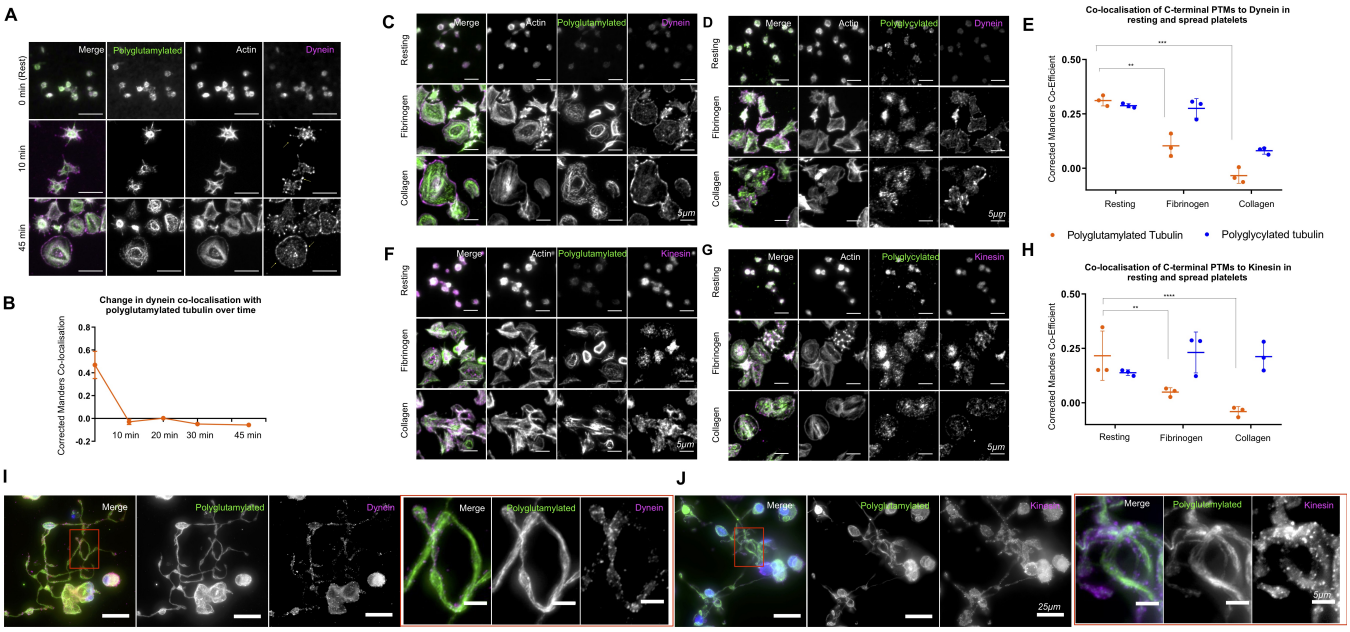

Fig. 5. Polyglutamylation regulates spatial distribution of motor proteins in platelets and MKs. (A, B) Quantification of the co-localisation of dynein with polyglutamylated tubulin over time shows a marked decrease in co-localisation on platelet activation. (C,D) In fibrinogen and collagen spread cells, axonemal dynein is observed on the periphery of the cell with no particular co-localisation evident with either polyglutamylated or polyglycylated tubulin. (E) Dynein co-localisation with polyglutamylated residues decreases dramatically on platelet spreading in both fibrinogen and collagen (** p = 0.0082 and p = *** 0.0004 respectively). No significant change in co-localisation with polyglycylated residues is observed. (F,G) Kinesin-1 staining is more diffuse throughout resting and spread platelets, on quantification (H) a loss of co-localisation with polyglutamylated tubulin is evident in fibrinogen and collagen spread cells (** p = 0.0017, **** p < 0.0001 respectively), with no significant change in co-localisation with polyglycylated tubulin. (I) Labelling of iPSC-MKs with polyglutamylated tubulin and axonemal dynein reveals the distribution of this motor along the length of the proplatelet shaft, (J) staining for kinesin-1 similarly shows the intimate association of this motor with the proplatelet shaft. Time course data: One-way ANOVA, other data Two-way ANOVA with uncorrected multiple comparisons performed, line of each plot represents mean and min/max values. *n* = 3. *10 μm scale bar.*

and the proplatelet extension suggests that axonemal dynein likely plays a role in this process.

E. MK and platelet polymodification is regulated through the expression of both modifying and reversing enzymes. Thus far we have reported a mechanism by which polyglutamylation and polyglycylation occur in mature and proplatelet forming MKs, followed by a change in distribution of these polymodifications (a reduction in polyglycylation) in the resting platelet, and finally an increase in the polyglutamylation of the marginal band on platelet activation and spreading. We hypothesise that the expression of cell specific subsets of effecting (Tubulin Tyrosine Like Ligase - TTLLs) and reversing (Cytoplasmic Carboxypeptidase - CCP) enzymes are required.

We designed a qRT-PCR panel to interrogate the expression of the 13 known mammalian TTLLs and 6 CCPs. We generated RNA from iPSC-MKs at different stages of the final terminal differentiation (Figures 6 A, S2A). Day 1 (d1) cells are representative of a pool of haematopoeitic stem cells (HSCs) and MK progenitors, while day 5 (d5) cells are comprised of 60% CD41/42b+ cells (Figures 6 A, S2 E). Finally, day 5 cells treated with heparin to induce proplatelet formation (d5 + Hep) are used to interrogate whether there is any specific up-regulation of TTLLs and/or CCPs on proplatelet formation (Figures 6 A, S2 D).

GAPDH housekeeping controls for each of the 3 samples (d1, d5, d5+Hep) show equivalent amplification of the housekeeping control, while results for TTLL family proteins show a number of enzymes expressed at different levels across the maturation of these cells (Figure 6 B,C). Candidate TTLLs observed in the initial endpoint PCR were taken forward for quantification across replicates generated from multiple differentiations, which included TTLLs 1, 2, 3, 4, 5, 6, 7, 10, and 13 (Figure 6 C,D). We find a significantly increased expression of TTLL1, TTLL2, TTLL4, and TTLL10 on proplatelet formation in cells treated with heparin (** p = 0.0081, * p = 0.0105, * p = 0.0260, *** p = 0.0004 respectively) (Figure 6 D).

CCP family enzymes were also found to be expressed in our maturing MKs, notably CCP1, 3, 4, 5, and 6 (Figure 6 E). Quantification across replicates revealed that CCP4 and 6 are up-regulated on proplatelet production (* p = 0.0130, *** p = 0.0009) (Figure 6 F).

To determine whether platelets demonstrate a difference in TTLL and CCP expression we repeated the PCR panel performed on maturing iPSC-MKs on platelet samples from 3 healthy donors. Each donor's platelets were either lysed in the resting state for RNA, or treated with CRP for 3 minutes to determine if there are changes in expression as a result of platelet activation. Interestingly, we found that none of the TTLLs and CCPs observed in iPSC MKs were consistently expressed across donors with the exception of TTLL7, a known polyglutamylase (Figure 6 G, complete gel in figure S6). No differences between resting and activated platelets were observed (Figure 6 G).

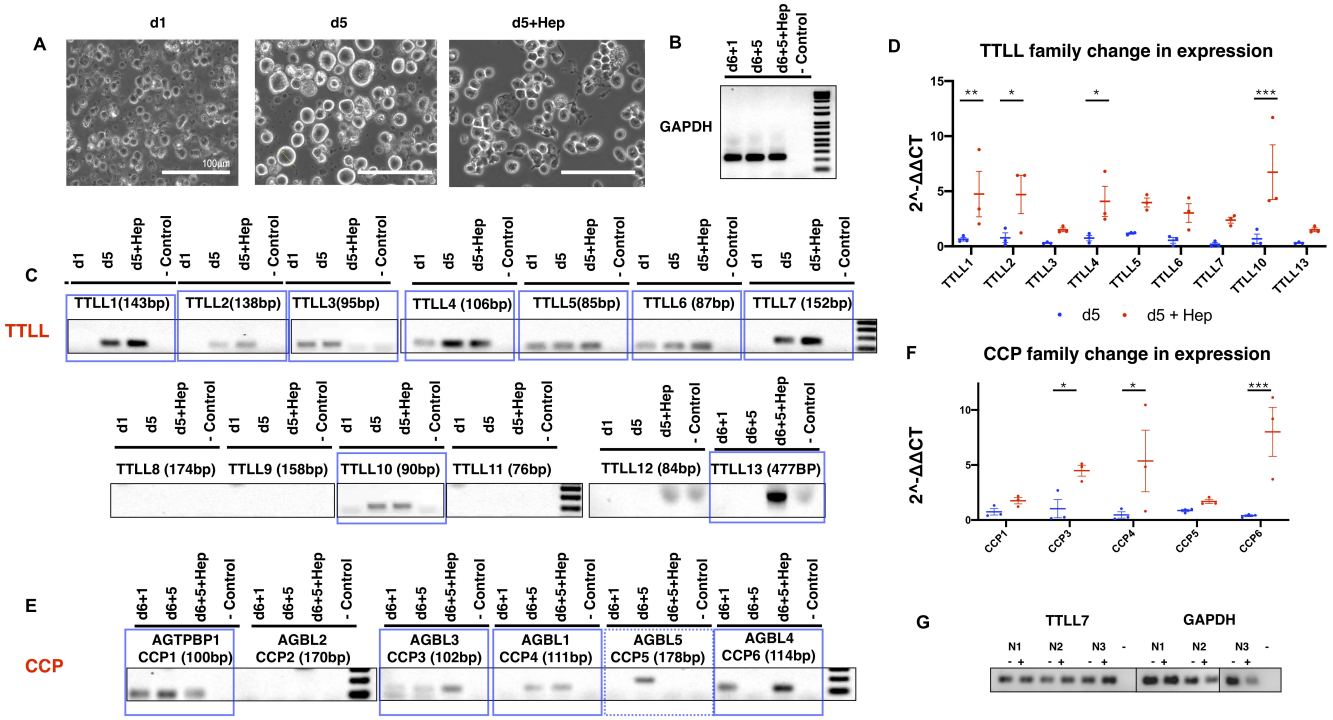

Fig. 6. iPSC-MKs and platelets differentially express TTLL and CCP enzymes to regulate polymodifications through MK maturation and platelet production. (A) RNA was generated from iPSC-MKs at different stages of terminal differentiation. Day 1 (d1) cells are comprised of HSCs and progenitors, while day 5 (d5) cells are primarily mature CD41/CD42b double positive cells. Finally, day 5 cells treated with heparin to induce proplatelet formation (d5 + Hep) were used to determine whether an upregulation of these enzymes is evident on platelet production. (B) Samples were amplified with housekeeping GAPDH primers to ensure that any differences in TTLL or CCP expression observed were not due to differences in RNA abundance or quality. (C) A number of TTLL family enzymes were observed, including TTLLs1, 2, 3, 4, 5, 6, 7, 10, and 13. Of these, a number appeared to be up-regulated in mature and proplatelet forming cells. (D) These samples were taken forward and expression was quantified over multiple differentiations using the $\delta\delta$CT method using d1 cells as controls to determine if there was any upregulation in TTLL expression on platelet production. TTLL 1, 2, 4, and 10 expression was found to be significantly upregulated on treatment with heparin (** p = 0.0081, * p = 0.0105, * p = 0.0260, *** p = 0.0004 respectively). (E) A similar panel was performed on CCP enzymes which reverse polymodifications, with expression of CCP1, 3, 4, 5, and 6 was observed. (F) Statistically significant upregulation of CCPs 4, and 6 were observed on proplatelet production (* p = 0.0130, *** p = 0.0009). (G) In resting (-) and CRP activated (+) platelets from 3 healthy donors TTLL7 was the only modifying enzyme found to be consistently expressed. (n = 3, S.D., Two-Way ANOVA with multiple comparisons performed. Complete unedited gels found in figures S5,S6.

F. TTLL10 mutations cause higher MPV and moderate to severe bleeding in 3 unrelated families. Our qRT-PCR screen reveals that a number of TTLL and CCPs are upregulated during the process of platelet production, including the monoglycylase TTLL3 and the polyglycylase TTLL10. 3 separate families were identified within the GAPP patient cohort with defects in the *TTLL10* gene (Figure 7A). Two of the three variants are frameshifts towards the N-terminus of the protein, preceding the ATP binding region (p.Pro15Argfs*38 and p.Val249Glyfs*57) (Figure 7 A). The final family has a missense p.Arg340Trp variant.

All three families report similar phenotypes, namely normal platelet counts, aggregation and secretion, but consistently high MPVs (normal ranges Mean Platelet Volume (fL) (7.83-10.5) and an established history of moderate to severe bleeding, including cutaneous bruising and menorrhagia (Figure 7 B). Interestingly, one of the patients (A 1:1) was further studied, and on platelet spreading on fibrinogen we observe a marked increase in platelet area compared to controls (Figure 7 C).

Discussion

Platelets and their progenitor cells, megakaryocytes, are a unique model for the study of the tubulin code. Like other specialist cells, they both express a lineage restricted isoform of β-tubulin (*TUBB1*) which is linked to disease pathologies when lost (inherited macrothrombocytopenias)(5, 18–20). However, unlike other specialist cells which exemplify the tubulin code, MKs and platelets execute markedly different functions despite their shared β-1 tubulin. MKs are the largest cell of the bone marrow, typified by a lobed, polyploid nucleus and the generation of long proplatelet extensions into the bone marrow sinusoids for the generation of platelets. Conversely platelets themselves are anucleate and the smallest circulating component of peripheral blood, classically involved in haemostasis and thrombosis, but with a myriad of other roles in wound healing, inflammation, and cancer progression. A key question is therefore how *TUBB1*, restricted to both cell types, helps these cells achieve markedly different morphologies and functions. We hypothesised that a system of polymodification (polyglutamylation and polyglycylation) targeting the glutamate rich C-terminus of this β-tubulin isoform, analogous to similar post-translational modifications demonstrated in cilia and neuronal cells, is a likely mechanism by which the interactions of β-1 tubulin with key motors are regulated in both MKs and platelets.

The study of this system is complicated by a lack of human cell lines which phenocopy primary MKs, namely in the

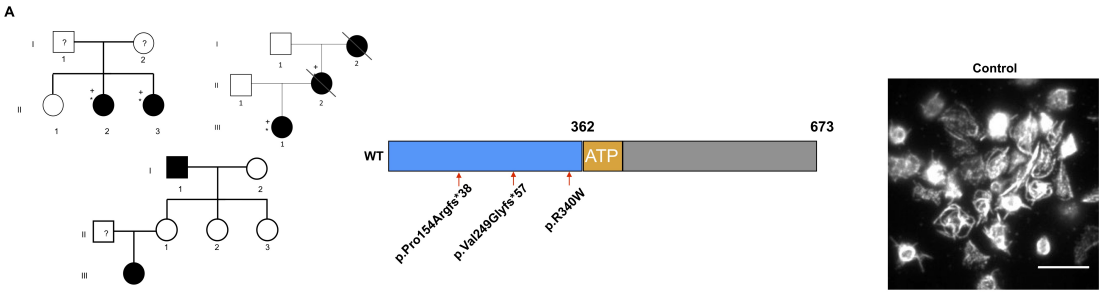

B

Individual	A	Sex	*TTLL10* Variant	Protein effect	Platelet count	IPF	MPV (fL)	Bleeding Phenotype	Functional Defect
A: I:1	34 '84	M	c.462delG	p.Pro155Arg fs*38	196	9	12.6	Unreported	Normal aggregometry, secretion.
A: I:2	31		WT		259	7.6	11.7	Menorrhagia	Normal aggregometry, secretion.
A: II:2	11 (2006)	F	c.462delG	p.Pro155Arg fs*38	246	4.2	11.3	Epistaxis, easy bruising and prolonged bleeding from minor	Normal aggregometry, secretion.
A: II:3	10 (2008)	F	c.462delG	p.Pro155Arg fs*38	329	5.6	12.1	Cutaneous bruising, easy bleeding	Normal aggregometry, secretion.
B: II:2	Deceased	F	c.745_746insG	p.Val249Glyf s*57	n/a	n/a	8.6	Easy bruising, menorrhagia	Normal aggregometry, secretion.
B: III:1	29	M	c.745_746insG	p.Val249Glyf s*57	n/a	n/a	9.4	Easy bruising, menorrhagia, bled from tooth extraction.	Normal aggregometry, secretion.
C: III:1	41	F	c.1018C>T	p.Arg340Trp	n/a	n/a	8.0	Cutaneous bruising, Menorrhagia, post partum haemorrhage x 2, bled	Normal aggregometry, secretion.

Fig. 7. TTLL10 deficient patients demonstrate platelets with a high MPV and a consistent history of bleeding. (A) Three unrelated families were identified within the GAPP cohort, two with frameshift truncations and one with a missense (p.Pro15Argfs*38, p.Val249Glyfs*57, and p.Arg340Trp respectively). (B) All three families present with normal platelet counts and function, but demonstrate an elevated mean platelet volume (MPV) and consistent histories of bleeding including cutaneous bruising and menorrhagia. (C) Patient A:1:1 volunteered to return and demonstrated abnormally large platelets on spreading on fibrinogen (tubulin staining, 10 μm scale bar).

generation of proplatelet extensions. Recent advances in the generation of MKs from iPSCs have allowed for the generation of large pools of mature CD41/42b+ cells, however few of these approaches have yielded large populations of MKs forming proplatelet networks equivalent to those produced by murine foetal liver cells for example (34, 35). In the study of the tubulin code and a system of post-translational modification, a species specific model is needed due to controversies regarding the functionality of particular modifying enzymes. TTLL10 for example, has both been reported as functionally redundant in humans by Rogowski *et al.*, and as an 'elongase' requiring the expression of an initiating enzyme (TTLL3) to enact its function as a polyglycylase (25, 28, 36). Therefore in this work we adapt an existing method of directed differentiation to produce large, proplatelet producing samples of iPSC-MKs for extensive immunfluorescence analysis of polymodifications and their association with motor proteins.

We report a system by which mature, CD42b+ iPSC-MKs demonstrate both polyglutamylation and polyglycylation. We do not observe any cells with proplatelet extensions absent of these polymodifications. Interestingly, we observe a markedly different distribution of these PTMs in the resting platelet, where polyglycylation is reduced and polyglutamylation is partially co-localised to the marginal band. On platelet activation, we observe a marked increase of polyglutamylation specific to the marginal band.

MK proplatelet extensions are known to be driven by a system of dynein mediated microtubule sliding, while the marginal band in a resting platelet has been shown to be maintained by the antagonistic movement of dynein and kinesin (13, 14, 32). Interestingly, polyglutamylation has been reported as a mechanism of altering motor protein processivity, with *in vitro* assays suggesting that polyglutamylation of β-tubulin isoforms like *TUBB1* and *TUBB3* accelerates these motors (29). We show a significant effect of polyglutamylation on the spatial localisation of dynein and kinesin, one which is not evidenced by polyglycylated residues, supporting *in vitro* assays which suggest that polyglutamylation is an accelerator of motor. Interestingly our data suggests that polyglycylation does not have such an effect on motor protein processivity. As both polyglutamylation and polyglycylation target the same substrate (a tubulin tail glutamate residue), it is likely that the competitive modification of these residues allows for the tight regulation of motor protein motility needed for proplatelet elongation. Interestingly the re-distribution of platelet polyglutamylation to the marginal band on platelet activation suggests that this is the mechanism by which the delicate balance of antagonistic motor protein function required to maintain the marginal band is disrupted.

This system of competitive polymodification is analogous to the post-translational modification of ciliated cells, and so we reasoned that axonemal dynein, an isoform of the motor exclusive to axonemes, may play a role in both platelet formation and activation (6, 37, 38). We find evidence of axonemal dynein on both proplatelet extensions and at the leading edge of spreading platelets. To our knowledge this is the first evidence of a functional role of axonemal dynein outside of classical ciliated structures.

Our data suggests a tightly regulated, reversible system of polymodification which must be mediated by the cell specific expression of TTLLs and CCPs. Interestingly, our expression profiles show a number of TTLLs and CCPs are expressed by MKs, while only the polyglutamylase TTLL7 is expressed by platelets, consistent with our finding that in the platelet activation results in polyglutamylation of the marginal band, but no change in polyglycylation. In MKs we find an increase in expression of two TTLLs known to be involved in glycylation - the initiase TTLL3 and the elongase TTLL10. As previously mentioned, TTLL10 is the source of some controversy in the field, with reports suggesting the acquisition of a mutation in humans which renders the enzyme non-functional. Our findings support a role of TTLL10 as a polyglycylase on co-expression with TTLL3 as reported by Ikegami *et al.* in cell lines through co-transfection experiments.

In mice with a variant of the deglutamylase CCP1, an increase in polyglutamylation results in the degeneration of photoreceptors in the retina(39). A series of human mutations in the deglutamylase CCP5 have been reported in patients with visual impairments(40, 41). A loss of glycylation has similarly been reported to affect ciliary function and length in mice, and a loss of this PTM in photoreceptors results in ciliary shortening and subsequent retinal degeneration in mouse models(8, 42). A knock-out model of TTLL3 results in a loss of glycylation and the development of tumours in the colon(43).

In the absence of established TTLL and *TUBB1* specific inhibitors, the role of the PTM of *TUBB1* in human physiology is best understood by disease models, and much of our current understanding of the tubulin code is derived from correlating the loss of PTMs with familial conditions (5). We identify two unrelated families with C-terminally oriented *TUBB1* variants, both presenting with macrothrombocytopenia and supporting a report from Fiore *et al.* suggesting that the loss of the C-terminus is causative of the disease.

TTLLs are generally, ubiquitously expressed and extensively required for the development of neuronal, retinal, and ciliated cells. Interestingly we identify 3 unrelated families with TTLL10 variants which result in an increase in platelet volume and an established history of bleeding and provides an invaluable insight to the potential role of polyglycylation in the context of platelet production and function. Our data suggests shows that both TTLL3 and TTLL10 are expressed in platelet producing MKs. Our patient cohort do not lose TTLL3 function, and as such the action of TTLL3 as an initiase will occupy glutamate residues which would otherwise be polyglutamylated. In these patients we likely see a loss of polyglycylation, but no co-incident increase in polyglutamylation due to the action of the initiase (TTLL3). As polyglutamylation and monoglycylation are unaffected, platelet counts (and production) are normal, however, affected individuals appear to have an increased platelet volume and bleeding, suggesting a role for the extended glycine tail in regulating platelet size, with a downstream effect on bleeding.

Conclusions

The 'tubulin code' posits that a tightly regulated system of post-translational modification as well as the lineage restricted expression of tubulin isoforms is required to drive unique cellular behaviours. This has been shown through both human disease states and mouse models which demonstrate that the loss of cell specific isoforms or particular regulatory enzymes can result in a range of neuronal dysfunctions, ciliopathies, abnormal spermatogenesis (or sperm function), and platelet defects. The loss of *TUBB1* has been established as causative of macrothrombocytopenias, however the mechanisms by which β-1 tubulin achieves the distinctive morphologies and functions of both MKs and platelets remains unknown.

Here we report a tightly regulated expression of glutamylating and glycylating enzymes through platelet production which drives the polyglutamylation and polyglycylation of MKs (Figure 8). These modifications are reduced in the terminal platelet which only expresses the polyglutamylase TTLL7, and on activation the marginal band becomes heavily polyglutamylated to drive motor protein mediated shape change. We show a role for axonemal dynein in proplatelet extension and platelet spreading, and report novel variants of *TTLL10* which result in bleeding through the loss of its' role as a polyglycylase. Ultimately the role of this system of polymodification is to fine tune the motility of motor proteins in both the MK and the platelet, allowing both cell types to achieve their unique functions.

This work supports the paradigm of a 'tubulin code', and suggests that there is likely a complex regulatory system upstream of TTLLs and CCPs within an MK and a platelet which drives these PTMs.

Materials and Methods

G. Platelet preparation. Whole blood was obtained for each experiment from healthy volunteers under the University of Birmingham's ERN 11-0175 license 'The regulation of activation of platelets'. Volumes of 25 mL were drawn from volunteers into sodium citrate. PRP (platelet-rich plasma) was generated by centrifugation of samples for 20 minutes at 200g. PRP was further spun to isolate platelets by centrifugation at 1,000g for 10 minutes with prostacyclin (0.1 μg/mL) and ACD. The resulting pellet was suspended in Tyrode's buffer prepared fresh, and pre-warmed at 37^0C (5mM glucose, 1mM MgCl2, 20mM HEPES, 12mM NaHCO3, 2.9 mM KCL, 0.34mM Na2HpO4, 129mM NaCL to a pH of 7.3). This suspension was spun again at 1,000g with prostacyclin at the same concentration before re-suspended to a final concentration of 2 x 10^8/mL. Platelets were left to rest for 30 minutes at room temperature before any further processing or treatment.

H. Platelet spreading. Resting platelets were fixed by preparing platelets at a concentration of 4 x 10^7/mL and mixing with equal volumes of 10% neutral buffered Formalin in a 15mL falcon tube. This mixture was inverted gently to mix

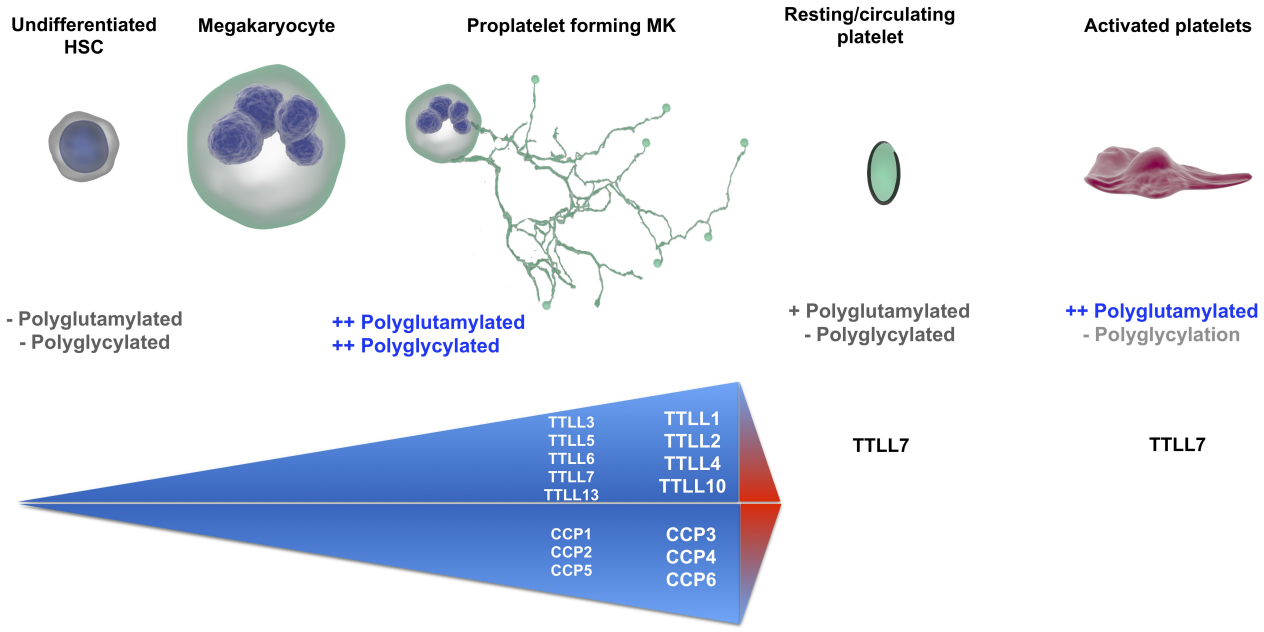

Fig. 8. A system of competitive polymodification of *TUBB1* driven by the expression of TTLL and CCP enzymes is required for platelet production and function. We observe a system by which as iPSC-MKs mature and express *TUBB1*, they acquire both polyglutamylated and polyglycylated tubulin which co-incides with an increase in the expression of glutamylating and glycylating TTLLs and reversing CCPs. A resting platelet is partially polyglutamylated, and on activation the marginal band is polyglutamylated to drive shape change and spreading throguh the action of TTLL7.

the sample, and left to incubate for 5 minutes before subsequently adding 300μL of the resulting fixed, resting platelets to coverslips coated in Poly-L-Lysine (Sigma). Cells were then spun down at 200g for 10 minutes.

Spreading was performed on human fibrinogen (Plasminogen, von Willebrand Factor and Fibronectin depleted - Enzyme Research Laboratories) and Horm collagen (Takeda). Coverslips were coated overnight at a concentration of 100 μg and 10μg/mL (fibrinogen and collagen) respectively, before blocking for 1 hour in denatured fatty acid free 1% BSA (Life Technologies). Finally coverslips were washed once with PBS before the addition of platelets. Unless otherwise stated (as in the time course experiment), platelets were spread for 45 minutes at 37^{0}C. Fixation for spread platelets was performed in formalin as for resting platelets for 10 minutes.

I. Immunofluorescence. After fixation platelets were washed twice with PBS before incubation in 0.1% Triton X-100 for 5 minutes. The subsequently permeabilised cells were washed twice with PBS before blocking in 2% Goat serum (Life Technologies) and 1% BSA (Sigma).

Fixed, permeablised, and blocked cells were then incubated with primary antibodies at a concentration of 1:500 unless otherwise stated. The following antibodies were used for experiments in this work: polyglutamylated tubulin (mouse monoclonal antibody, clone B3 T9822, Sigma), pan-polyglycylated antibody (mouse monoclonal antibody, AXO49, MABS276 Millipore), monoglycylated antibody (AXO 962 mouse monoclonal MABS277, EMD Millipore), kinesin-1 (rabbit monoclonal to KIF1B ab 167429, abcam), axonemal dynein, β-tubulin (Rabbit polyclonal PA5-16863 tyrosinated tubulin (rabbit monoclonal antibody, clone YL1/2, MAB1864, EMD Millipore), acetylated tubulin (Lys40, 6-11B-1, mouse monoclonal antibody, Cell Signalling Technology). DNAL1 antibody (PA5-30643 Invitrogen).

After a 1 hour incubation in the relevant mix of primary antibodies. Cells were washed twice with PBS before incubation in secondary antibodies (Alexa-568-phalloidin, anti-rabbit Alexa-647, anti-mouse Alexa-588) for one hour at a dilution of 1:300 in PBS.

J. Stem Cell Culture. Gibco human episomal induced pluripotent stem cell line was purchased from Thermo Scientific and cultured on Geltrex basement membrane in Stem-Flex medium (Thermo Scientific).

Routine passaging was performed using EDTA (Sigma), with single cell seeding performed for transfection and attempted clonal isolation through the use of TryplE (Thermo Scientific). Briefly, cells were washed twice with PBS and once with either EDTA (for clump passaging) or TrypLE (for single cell) before incubation in 1mL relevant detachment media for 3 minutes at 37°C.

For clump passaging, EDTA was removed and 1mL of Stem-Flex added. Cells were detached by triurtating media onto the bottom of the well and subsequently adding the required volume to fresh media (in a new, GelTrex coated plate).

For single cell seeding, TrypLE was diluted in 2mL Stem-Flex and the solution added to a 15mL falcon tube for centrifugation at 200g for 4 minutes. The supernatant was then discarded and the cell pellet resuspended in the required volume.

K. iPSC MK differentiation. iPSC differentiation to mature, proplatelet forming megakaryocytes was performed us-

ing a protocol based on work published by Feng *et al.*(35). To summarise, cells were detached by clump passaging and seeded on dishes coated with Collagen Type IV (Advanced Biomatrix) at 5μg/cm^2. Cells were seeded overnight with RevitaCell to support survival on the new basement substrate. To begin the protocol cells were washed twice and incubated in phase I medium comprised of APELII medium (Stem Cell Technologies) supplemented with BMP-4 (Thermo Scientific), FGF-β, and VEGF (Stem Cell Technologies) at 50ng/mL each. Cells were incubated at 5% oxygen for the first four days of the protocol before being placed in a standard cell culture incubator for a further two days in freshly made phase I medium.

At day 6 of the protocol cells were incubated in phase II media comprised of APELII, TPO (25 ng/mL), SCF (25 ng/mL), Flt-3 (25ng/mL), Interleukin-3 (10ng/mL), Interleukin-6 (10 ng/mL) and Heparin (5 U/mL) (all supplied by Stem Cell Technologies). Each day in phase II media suspension cells were spun down at 400g for 5 minutes and frozen in 10% FBS/DMSO. After 5 days of collection, all frozen cells were thawed for terminal differentiation. Terminal differentiation was performed by incubating cells in StemSpan II with heparin (5U/mL) and Stem Cell Technologies Megakaryocyte Expansion supplement on low attachment dishes (Corning).

L. Microscopy. Images were acquired using an Axio Observer 7 inverted epifluorescence microscope (Carl Zeiss) with Definite Focus 2 autofocus, 63x 1.4 NA oil immersion objective lens, Colibri 7 LED illumination source, Hammamatsu Flash 4 V2 sCMOS camera, Filter sets 38, 45HQ and 50 for Alexa488, Alexa568 and Alexa647 respectively and DIC optics. LED power and exposure time were chosen as appropriate for each set of samples but kept the same within each experiment. Using Zen 2.3 Pro software, five images were taken per replicate, either as individual planes (spread platelets) or representative Z-stacks (resting platelets).

M. Image and statistical analysis. Statistical analysis was performed using GraphPad PRISM 7. Image analysis was performed using a custom segmentation algorithm developed by Jeremy Pike. Briefly, the actin channel from resting and spread platelet images was used to train Ilastik classifiers (approximately 6 images per condition) for segmentation based on this channel. This was incorporated into a Knime workflow which would run images through the classifier to generated segmented binaries in which co-localisation and fluorescence intensity statistics were calculated. For the data presented in this manuscript, M1 (a corrected Mander's co-efficient to channel 1) was used to determine the co-localisation of PTMs to tubulin, and an M2 value (corrected Mander's co-efficient to channel 2) was used to calculate the co-localisation of motor proteins to PTMs of interest.

N. Quantitative Real Time PCR (qRT-PCR). To determine whether the 13 mammalian TTLLs and 6 CCPs were expressed in iPSC-MKs at the different stages of differentiation (day 1, day 5 and day 5 +heparin) a qRT-PCR panel was developed using TaqMan technology and an ABI 7900 HT analyser (Applied Biosystems, Warrington, UK). RNA samples were isolated and reverse-transcribed and amplified with the relevant primers using SYBR-Green based technology (Power SYBR(r) Master Mix, Life Technologies). Total RNA was extracted from iPSC cells using the NucleoSpin RNA kit (Machery-Nagel) and cDNA was synthesized using the High-Capacity cDNA Reverse Transcription Kit (Life Technologies). qRT-PCR was performed on all the TTLL/CCP fragments generated from primers designed in table x and the housekeeping control GAPDH (GAPDHFOR $5' - GAAGGTGAAGGTCGGAGT - 3'$ and GAPDHREV $5'GAAGATGGTGATGGGATTTC - 3'$). Each reaction was set up in triplicate including a non-template control. Expression was analysed using the CT method using D1 undifferentiated cells as a control. A full list of primer sequences has been uploaded as figure S4.

O. *TUBB1* Homology Modelling. Homology models of TUBB1 WT and mutations were made using SWISS MODEL software (44–47), using the solved TUBB3 heterodimer as a template (PDB: 5IJ0 (48)). TUBB1 and TUBB3 share approximately 80% sequence identity, and the model created corresponds to residues 1-425 of TUBB1.

ACKNOWLEDGEMENTS

We thank the families for providing samples and our clinical and laboratory colleagues for their help. This work was supported by the British Heart Foundation (PG/13/36/30275; FS/13/70/30521; FS/15/18/31317). The authors would like to thank the TechHub and COMPARE Core facilities at the University of Birmingham. We thank Professor Steve Watson for his ongoing support and invaluable mentorship.

Bibliography

1. Sudarshan Gadadhar, Satish Bodakuntla, Kathiresan Natarajan, and Carsten Janke. The tubulin code at a glance. *J Cell Sci*, 130(8):1347–1353, Apr 2017. doi: 10.1242/jcs.199471.
2. Sudarshan Gadadhar, Hala Dadi, Satish Bodakuntla, Anne Schnitzler, Ivan Bièche, Filippo Rusconi, and Carsten Janke. Tubulin glycylation controls primary cilia length. *J Cell Biol*, 216(9):2701–2713, 09 2017. doi: 10.1083/jcb.201612050.
3. Sudarshan Gadadhar, Satish Bodakuntla, Kathiresan Natarajan, and Carsten Janke. The tubulin code at a glance. *J Cell Sci*, 130(8):1347–1353, 04 2017. doi: 10.1242/jcs.199471.
4. Richard F Ludueña. A hypothesis on the origin and evolution of tubulin. *Int Rev Cell Mol Biol*, 302:41–185, 2013. doi: 10.1016/B978-0-12-407699-0.00002-9.
5. Maria M Magiera, Puja Singh, and Carsten Janke. Snapshot: Functions of tubulin post-translational modifications. *Cell*, 173(6):1552–1552.e1, May 2018. doi: 10.1016/j.cell.2018.05.032.
6. Dorota Wloga, Ewa Joachimiak, Panagiota Louka, and Jacek Gaertig. Posttranslational modifications of tubulin and cilia. *Cold Spring Harb Perspect Biol*, 9(6), Jun 2017. doi: 10.1101/cshperspect.a028159.
7. Jeremy F Reiter and Michel R Leroux. Genes and molecular pathways underpinning ciliopathies. *Nat Rev Mol Cell Biol*, 18(9):533–547, Sep 2017. doi: 10.1038/nrm.2017.60.
8. Montserrat Bosch Grau, Christel Masson, Sudarshan Gadadhar, Cecilia Rocha, Olivia Tort, Patricia Marques Sousa, Sophie Vacher, Ivan Bieche, and Carsten Janke. Alterations in the balance of tubulin glycylation and glutamylation in photoreceptors leads to retinal degeneration. *J Cell Sci*, 130(5):938–949, Mar 2017. doi: 10.1242/jcs.199091.
9. Koji Ikegami, Showbu Sato, Kenji Nakamura, Lawrence E Ostrowski, and Mitsutoshi Setou. Tubulin polyglutamylation is essential for airway ciliary function through the regulation of beating asymmetry. *Proc Natl Acad Sci U S A*, 107(23):10490–5, Jun 2010. doi: 10.1073/pnas.1002128107.
10. Hui-Yuan Wu, Peng Wei, and James I Morgan. Role of cytosolic carboxypeptidase 5 in neuronal survival and spermatogenesis. *Sci Rep*, 7:41428, 01 2017. doi: 10.1038/srep41428.
11. P Vogel, G Hansen, G Fontenot, and R Read. Tubulin tyrosine ligase-like 1 deficiency results in chronic rhinosinusitis and abnormal development of spermatid flagella in mice. *Vet Pathol*, 47(4):703–12, Jul 2010. doi: 10.1177/0300985810363485.
12. Serge Dmitrieff, Adolfo Alsina, Aastha Mathur, and François J Nédélec. Balance of microtubule stiffness and cortical tension determines the size of blood cells with marginal band across species. *Proc Natl Acad Sci U S A*, 114(17):4418–4423, Apr 2017. doi: 10.1073/pnas.1618041114.
13. Boubou Diagouraga, Alexei Grichine, Arnold Fertin, Jin Wang, Saadi Khochbin, and Karin Sadoul. Motor-driven marginal band coiling promotes cell shape change during platelet activation. *J Cell Biol*, 204(2):177–85, Jan 2014. doi: 10.1083/jcb.201306085.
14. K Sadoul. New explanations for old observations: marginal band coiling during platelet activation. *J Thromb Haemost*, 13(3):333–46, Mar 2015. doi: 10.1111/jth.12819.

15. Natalie S Poulter and Steven G Thomas. Cytoskeletal regulation of platelet formation: Coordination of f-actin and microtubules. *Int J Biochem Cell Biol*, 66:69–74, Sep 2015. doi: 10.1016/j.biocel.2015.07.008.
16. Kellie R Machlus and Joseph E Italiano, Jr. The incredible journey: From megakaryocyte development to platelet formation. *J Cell Biol*, 201(6):785–96, Jun 2013. doi: 10.1083/jcb.201304054.
17. H D Schwer, P Lecine, S Tiwari, J E Italiano, Jr, J H Hartwig, and R A Shivdasani. A lineage-restricted and divergent beta-tubulin isoform is essential for the biogenesis, structure and function of blood platelets. *Curr Biol*, 11(8):579–86, Apr 2001.
18. Shinji Kunishima, Ryoji Kobayashi, Tomohiko J Itoh, Motohiro Hamaguchi, and Hidehiko Saito. Mutation of the beta1-tubulin gene associated with congenital macrothrombocytopenia affecting microtubule assembly. *Blood*, 113(2):458–61, Jan 2009. doi: 10.1182/blood-2008-06-162610.
19. Shinji Kunishima, Satoshi Nishimura, Hidenori Suzuki, Masue Imaizumi, and Hidehiko Saito. Tubb1 mutation disrupting microtubule assembly impairs proplatelet formation and results in congenital macrothrombocytopenia. *Eur J Haematol*, 92(4):276–82, Apr 2014. doi: 10.1111/ejh.12252.
20. M Fiore, C Goulas, and X Pillois. A new mutation in tubb1 associated with thrombocytopenia confirms that c-terminal part of β1-tubulin plays a role in microtubule assembly. *Clin Genet*, 91(6):924–926, Jun 2017. doi: 10.1111/cge.12879.
21. Sunita Patel-Hett, Jennifer L Richardson, Harald Schulze, Ksenija Drabek, Natasha A Isaac, Karin Hoffmeister, Ramesh A Shivdasani, J Chloë Bulinski, Niels Galjart, John H Hartwig, and Joseph E Italiano, Jr. Visualization of microtubule growth in living platelets reveals a dynamic marginal band with multiple microtubules. *Blood*, 111(9):4605–16, May 2008. doi: 10.1182/blood-2007-10-118844.
22. Kathiresan Natarajan, Sudarshan Gadadhar, Judith Souphron, Maria M Magiera, and Carsten Janke. Molecular interactions between tubulin tails and glutamylases reveal determinants of glutamylation patterns. *EMBO Rep*, 18(6):1013–1026, Jun 2017. doi: 10.15252/embr.201643751.
23. A Wolff, B de Néchaud, D Chillet, H Mazarguil, E Desbruyères, S Audebert, B Eddé, F Gros, and P Denoulet. Distribution of glutamylated alpha and beta-tubulin in mouse tissues using a specific monoclonal antibody, gt335. *Eur J Cell Biol*, 59(2):425–32, Dec 1992.
24. Dorota Wloga, Danielle M Webster, Krzysztof Rogowski, Marie-Hélène Bré, Nicolette Levilliers, Maria Jerka-Dziadosz, Carsten Janke, Scott T Dougan, and Jacek Gaertig. Ttll3 is a tubulin glycine ligase that regulates the assembly of cilia. *Dev Cell*, 16(6):867–76, Jun 2009. doi: 10.1016/j.devcel.2009.04.008.
25. Krzysztof Rogowski, François Juge, Juliette van Dijk, Dorota Wloga, Jean-Marc Strub, Nicolette Levilliers, Daniel Thomas, Marie-Hélène Bré, Alain Van Dorsselaer, Jacek Gaertig, and Carsten Janke. Evolutionary divergence of enzymatic mechanisms for posttranslational polyglycylation. *Cell*, 137(6):1076–87, Jun 2009. doi: 10.1016/j.cell.2009.05.020.
26. Alu Konno, Koji Ikegami, Yoshiyuki Konishi, Hyun-Jeong Yang, Manabu Abe, Maya Yamazaki, Kenji Sakimura, Ikuko Yao, Kogiku Shiba, Kazuo Inaba, and Mitsutoshi Setou. Ttll9-/- mice sperm flagella show shortening of doublet 7, reduction of doublet 5 polyglutamylation and a stall in beating. *J Cell Sci*, 129(14):2757–66, 07 2016. doi: 10.1242/jcs.185983.
27. R J Mullen, E M Eicher, and R L Sidman. Purkinje cell degeneration, a new neurological mutation in the mouse. *Proc Natl Acad Sci U S A*, 73(1):208–12, Jan 1976.
28. Koji Ikegami, Robb L Heier, Midori Taruishi, Hiroshi Takagi, Masahiro Mukai, Shuichi Shimma, Shu Taira, Ken Hatanaka, Nobuhiro Morone, Ikuko Yao, Patrick K Campbell, Shigeki Yuasa, Carsten Janke, Grant R Macgregor, and Mitsutoshi Setou. Loss of alpha-tubulin polyglutamylation in rosa22 mice is associated with abnormal targeting of kif1a and modulated synaptic function. *Proc Natl Acad Sci U S A*, 104(9):3213–8, Feb 2007. doi: 10.1073/pnas.0611547104.
29. Minhajuddin Sirajuddin, Luke M Rice, and Ronald D Vale. Regulation of microtubule motors by tubulin isotypes and post-translational modifications. *Nat Cell Biol*, 16(4):335–44, Apr 2014. doi: 10.1038/ncb2920.
30. Juliette van Dijk, Guillaume Bompard, Julien Cau, Shinji Kunishima, Gabriel Rabeharivelo, Julio Mateos-Langerak, Chantal Cazevieille, Patricia Cavelier, Brigitte Boizet-Bonhoure, Claude Delsert, and Nathalie Morin. Microtubule polyglutamylation and acetylation drive microtubule dynamics critical for platelet formation. *BMC Biol*, 16(1):116, 10 2018. doi: 10.1186/s12915-018-0584-6.
31. Koji Ikegami and Mitsutoshi Setou. Ttll10 can perform tubulin glycylation when co-expressed with ttll8. *FEBS Lett*, 583(12):1957–63, Jun 2009. doi: 10.1016/j.febslet.2009.05.003.
32. Markus Bender, Jonathan N Thon, Allen J Ehrlicher, Stephen Wu, Linas Mazutis, Emoke Deschmann, Martha Sola-Visner, Joseph E Italiano, and John H Hartwig. Microtubule sliding drives proplatelet elongation and is dependent on cytoplasmic dynein. *Blood*, 125(5):860–8, Jan 2015. doi: 10.1182/blood-2014-09-600858.
33. Frédéric Adam, Alexandre Kauskot, Mathieu Kurowska, Nicolas Goudin, Isabelle Munoz, Jean-Claude Bordet, Jian-Dong Huang, Marijke Bryckaert, Alain Fischer, Delphine Borgel, Geneviève de Saint Basile, Olivier D Christophe, and Gaël Ménasché. Kinesin-1 is a new actor involved in platelet secretion and thrombus stability. *Arterioscler Thromb Vasc Biol*, 38(5):1037–1051, May 2018. doi: 10.1161/ATVBAHA.117.310373.
34. Thomas Moreau, Amanda L Evans, Louella Vasquez, Marloes R Tijssen, Ying Yan, Matthew W Trotter, Daniel Howard, Maria Colzani, Meera Arumugam, Wing Han Wu, Amanda Dalby, Riina Lampela, Guenaelle Bouet, Catherine M Hobbs, Dean C Pask, Holly Payne, Tatyana Ponomaryov, Alexander Brill, Nicole Soranzo, Willem H Ouwehand, Roger A Pedersen, and Cedric Ghevaert. Large-scale production of megakaryocytes from human pluripotent stem cells by chemically defined forward programming. *Nat Commun*, 7:11208, Apr 2016. doi: 10.1038/ncomms11208.
35. Qiang Feng, Namrata Shabrani, Jonathan N Thon, Hongguang Huo, Austin Thiel, Kellie R Machlus, Kyungho Kim, Julie Brooks, Feng Li, Chenmei Luo, Erin A Kimbrel, Jiwu Wang, Kwang-Soo Kim, Joseph Italiano, Jaehyung Cho, Shi-Jiang Lu, and Robert Lanza. Scalable generation of universal platelets from human induced pluripotent stem cells. *Stem Cell Reports*, 3(5):817–31, Nov 2014. doi: 10.1016/j.stemcr.2014.09.010.
36. Sou Nakamura, Naoya Takayama, Shinji Hirata, Hideya Seo, Hiroshi Endo, Kiyosumi Ochi, Ken-ichi Fujita, Tomo Koike, Ken-ichi Harimoto, Takeaki Dohda, Akira Watanabe, Keisuke Okita, Nobuyasu Takahashi, Akira Sawaguchi, Shinya Yamanaka, Hiromitsu Nakauchi, Satoshi Nishimura, and Koji Eto. Expandable megakaryocyte cell lines enable clinically applicable generation of platelets from human induced pluripotent stem cells. *Cell Stem Cell*, 14(4):535–48, Apr 2014. doi: 10.1016/j.stem.2014.01.011.
37. Robert O'Hagan, Malan Silva, Ken C Q Nguyen, Winnie Zhang, Sebastian Bellotti, Yasmin H Ramadan, David H Hall, and Maureen M Barr. Glutamylation regulates transport, specializes function, and sculpts the structure of cilia. *Curr Biol*, 27(22):3430–3441.e6, Nov 2017. doi: 10.1016/j.cub.2017.09.066.
38. Dorota Wloga, Drashti Dave, Jennifer Meagley, Krzysztof Rogowski, Maria Jerka-Dziadosz, and Jacek Gaertig. Hyperglutamylation of tubulin can either stabilize or destabilize microtubules in the same cell. *Eukaryot Cell*, 9(1):184–93, Jan 2010. doi: 10.1128/EC.00176-09.
39. Miguel Marchena, Juan Lara, José Aijón, Francisco Germain, Pedro de la Villa, and Almudena Velasco. The retina of the pcd/pcd mouse as a model of photoreceptor degeneration. a structural and functional study. *Exp Eye Res*, 93(5):607–17, Nov 2011. doi: 10.1016/j.exer.2011.07.010.
40. Galuh D N Astuti, Gavin Arno, Sarah Hull, Laurence Pierrache, Hanka Venselaar, Keren Carss, F Lucy Raymond, Rob W J Collin, Sultana M H Faradz, L Ingeborgh van den Born, Andrew R Webster, and Frans P M Cremers. Mutations in agbl5, encoding α-tubulin deglutamylase, are associated with autosomal recessive retinitis pigmentosa. *Invest Ophthalmol Vis Sci*, 57(14):6180–6187, Nov 2016. doi: 10.1167/iovs.16-20148.
41. Sandra E Branham, Sara J Wright, Aaron Reba, and C Randal Linder. Genome-wide association study of arabidopsis thaliana identifies determinants of natural variation in seed oil composition. *J Hered*, 107(3):248–56, 05 2016. doi: 10.1093/jhered/esv100.
42. Montserrat Bosch Grau, Christel Masson, Sudarshan Gadadhar, Cecilia Rocha, Olivia Tort, Patricia Marques Sousa, Sophie Vacher, Ivan Bieche, and Carsten Janke. Alterations in the balance of tubulin glycylation and glutamylation in photoreceptors leads to retinal degeneration. *J Cell Sci*, 130(5):938–949, 03 2017. doi: 10.1242/jcs.199091.
43. Cecilia Rocha, Laura Papon, Wulfran Cacheux, Patricia Marques Sousa, Valeria Lascano, Olivia Tort, Tiziana Giordano, Sophie Vacher, Benedicte Lemmers, Pascale Mariani, Didier Meseure, Jan Paul Medema, Ivan Bièche, Michael Hahne, and Carsten Janke. Tubulin glycylases are required for primary cilia, control of cell proliferation and tumor development in colon. *EMBO J*, 33(19):2247–60, Oct 2014. doi: 10.15252/embj.201488466.
44. Andrew Waterhouse, Christine Rempfer, Florian T Heer, Gabriel Studer, Gerardo Tauriello, Lorenza Bordoli, Martino Bertoni, Rafal Gumienny, Rosalba Lepore, Stefan Bienert, Tjaart A P de Beer, and Torsten Schwede. SWISS-MODEL: homology modelling of protein structures and complexes. *Nucleic Acids Research*, 46(W1):W296–W303, 05 2018. ISSN 0305-1048. doi: 10.1093/nar/gky427.
45. Andrew Waterhouse, Gabriel Studer, Gerardo Tauriello, Lorenza Bordoli, Stefan Bienert, Tjaart A. P. de Beer, and Torsten Schwede. The SWISS-MODEL Repository—new features and functionality. *Nucleic Acids Research*, 45(D1):D313–D319, 11 2016. ISSN 0305-1048. doi: 10.1093/nar/gkw1132.
46. Nicolas Guex, Manuel C. Peitsch, and Torsten Schwede. Automated comparative protein structure modeling with swiss-model and swiss-pdbviewer: A historical perspective. *ELECTROPHORESIS*, 30(S1):S162–S173. doi: 10.1002/elps.200900140.
47. Marco Biasini, Pascal Benkert, and Torsten Schwede. Toward the estimation of the absolute quality of individual protein structure models. *Bioinformatics*, 27(3):343–350, 12 2010. ISSN 1367-4803. doi: 10.1093/bioinformatics/btq662.
48. Shih-Chieh Ti, Melissa C. Pamula, Stuart C. Howes, Christian Duellberg, Nicholas I. Cade, Ralph E. Kleiner, Scott Forth, Thomas Surrey, Eva Nogales, and Tarun M. Kapoor. Mutations in human tubulin proximal to the kinesin-binding site alter dynamic instability at microtubule plus- and minus-ends. *Developmental Cell*, 37(1):72 – 84, 2016. ISSN 1534-5807. doi: https://doi.org/10.1016/j.devcel.2016.03.003.

Supplementary Figures and Tables

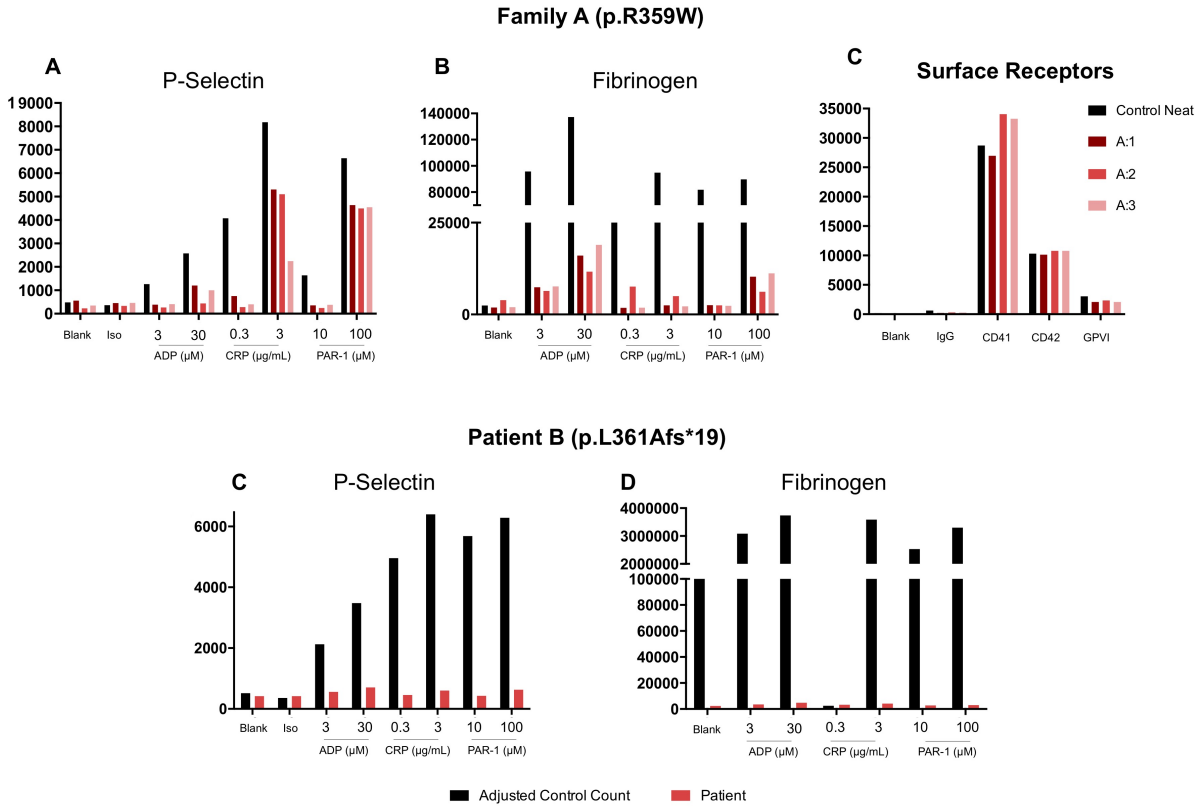

Fig. S1. Patient flow cytometry data reveals secondary defects. The GAPP project collects phenotypic data on patient recruitment, allowing for the assessment of secondary defects through FACS screening.(A) Patient B shows a marked reduction in P-selectin surface expression and (B) fibrinogen uptake compared to controls. (C) Individuals from family A show a reduction in P-selectin at both doses of CRP, low dose CRP, and low dose PAR-1. (D) Patients similarly show a reduction in fibrinogen uptake compared to controls, but show no difference in (E) surface marker expression.

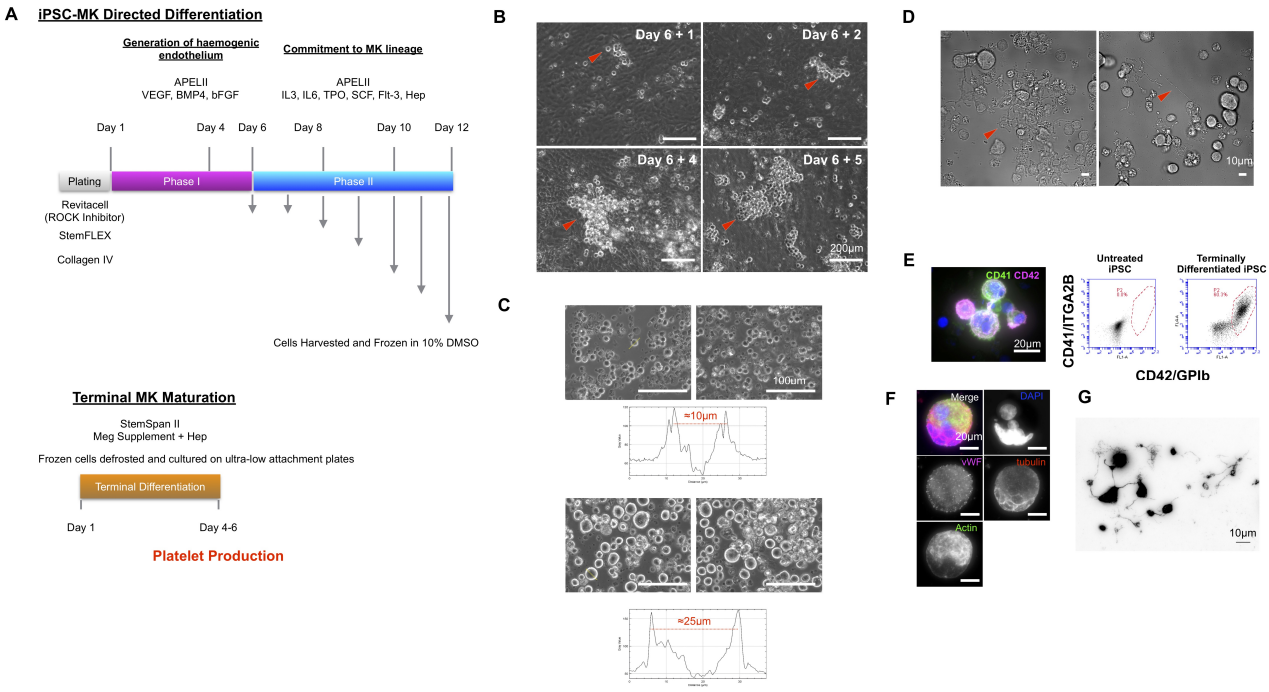

Fig. S2. Directed differentiation of iPSC to proplatelet forming MKs. (A) A 3 stage protocol was adapted from a method previously published by Feng *et al.*. Briefly, iPSC were clump passaged on to collagen IV coated plates and incubated in RevitaCell overnight before beginning Phase I of the differentiation. Phase I involves a 4 day incubation at 5% O_2 in APEL2 media supplemented with 50ng of BMP4, VEGF, and FGF2, after which fresh media was added and cells were incubated for 2 more days at normoxic conditions. Phase II of the protocol involved incubation in APEL2 supplemented with IL3, IL6, Flt-3, hSCF, TPO, heparin, during which time cells were harvested and frozen every 48 hours and fresh media added. Finally, harvested cells were thawed and incubated in StemSpan II medium with MK supplement for 5 days before samples were prepared for downstream assays (immunofluorescence, RT-PCR etc.). (B) During Phase II of the differentiation, progressively larger numbers of blast like cells are observed emerging from a layer of haemogenic endothelium. (C) During Phase III of the differentiation, cells grow from progenitors and blast like cells approximately 10 μm in size to large, mature MKs ranging in 25-40 μm in size. (D) At day 5, on treatment with Y-27632 and heparin, cells form elaborate proplatelet networks. (E) 60% of terminally (Phase III) differentiated cells are CD41 and CD42 double positive and on staining demonstrate (G) a mix of ploidies and proplatelet networks consistent with mature platelet producing MKs.

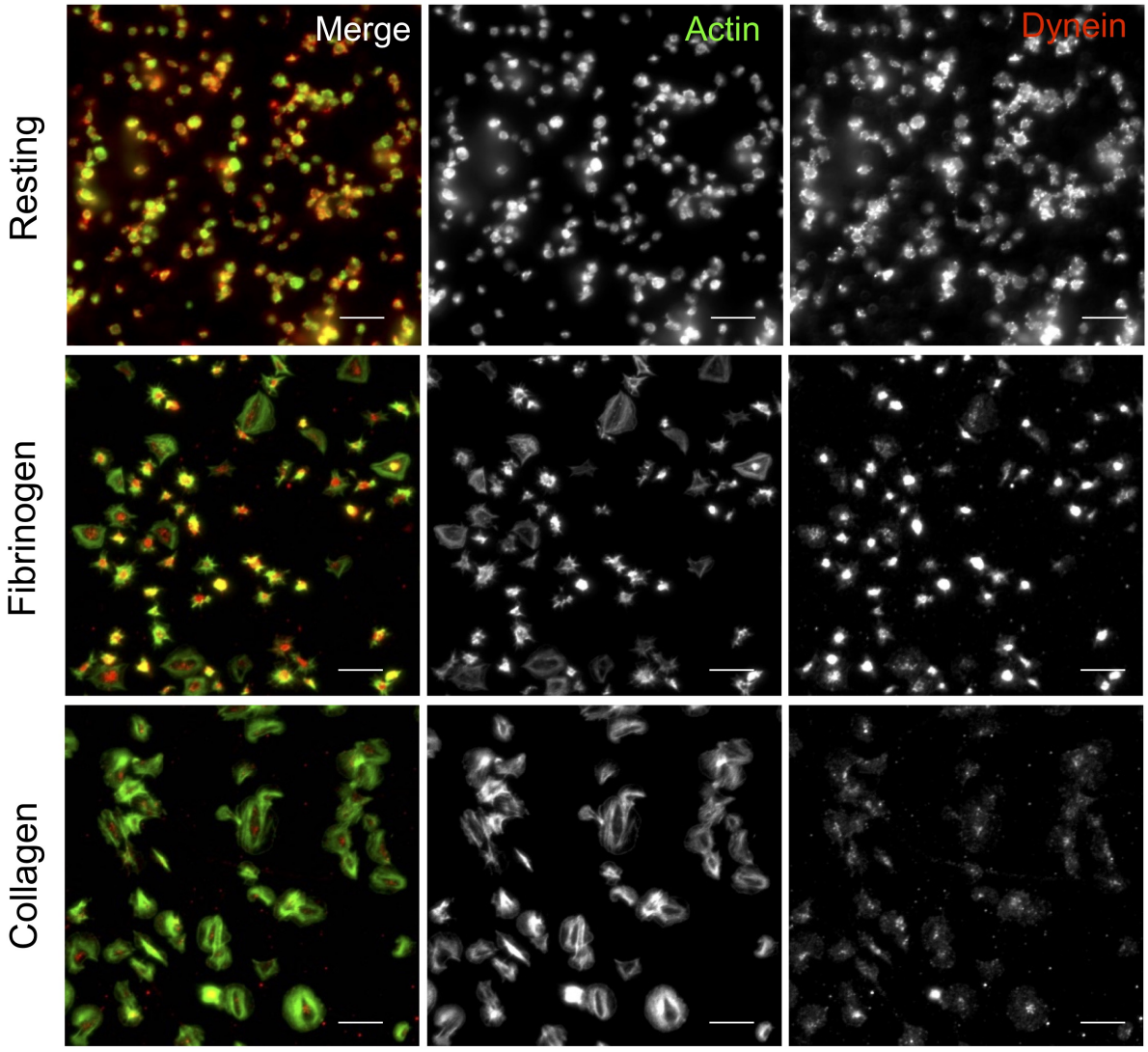

Fig. S3. Staining of Cytoplasmic Dynein in resting and Spread Platelets. Resting and spread human donor platelets were stained for cytoplasmic dynein to compare the distribution of this isoform of the motor protein to axonemal dynein. While axonemal dynein is primarily found on the edge of spreading cells, cytoplasmic dynein is found at the centre of spread cells, suggesting that the axonemal variant is involved in platelet spreading and activation.

Name	Sequence : (5' to 3')	Fragment Size	Name	Sequence : (5' to 3')	Fragment Size
FH1_TTLL1	AGTCAACCATTTTCCAAACC	143 bp	FH1_TTLL11	ATTTGTTTATCCGGTTCCTG	76 bp
RH1_TTLL1	AGTCCAGATAGAGGTATTTTCC		RH1_TTLL11	CTCCTTATGAAGGTACGAAAG	
FH1_TTLL2	GCCTTTACCCTTAACATTCC	138 bp	FH1_TTLL12	CATTCTGGAGGAAAACAAGG	84 bp
RH1_TTLL2	TTTCTTCTTCTCCAGTGTTG		RH1_TTLL12	GTGTAGACCTTGAAGATGTG	
FH1_TTLL3	AAGCCTTCATAGAGGACTTC	95 bp	FH1_TTLL13	ACCTGACCAACTATGCTATC	477 bp
RH1_TTLL3	TACTGCCTGAATAGGGTATG		RH1_TTLL13	TGGTTTTGATGATGATGTCC	
FH1_TTLL4	GAAGCTAAACCATTTCCCAG	106 bp	FH1_AGTPBP1 (CCP1)	AAAAACAAATGCCAGGAGAG	100 bp
RH1_TTLL4	GAAACTGAACTCCTTCTTGC		FH1_AGTPBP1 (CCP1)	CATGTTTCTATGCCGGTTATC	
FH1_TTLL5	AATTCATATTCGAAGGACCG	85 bp	FH1_AGBL2 (CCP2)	GGCCTATCAGTTTATCTTCAG	170 bp
RH1_TTLL5	GATTGTTGATCAGGTAGACG		RH1_AGBL2 (CCP2)	ATCTGTAATCCCAGCTACTC	
FH1_TTLL6	AAGCCCTTTATCATTGATGG	87 bp	FH1_AGBL3 (CCP3)	GAAGAGCAAAGAAGGAACAG	102 bp
RH1_TTLL6	GTACACAAAAATCCTGAGAGG		RH1_AGBL3 (CCP3)	TTGTTACCCAGAGTAGATCC	
FH1_TTLL7	CAGAATTGGTGGTAAAGACC	152 bp	FH1_AGBL1 (CCP4)	AGATGATGACTTGGAAACAG	111 bp
RH1_TTLL7	CCATGGCTTTAGTTTTCTATCC		RH1_AGBL1 (CCP4)	CTATAGGAGAGCTCAAGACAC	
FH1_TTLL8	AACAAGGAATTTCCCAAGAC	174 bp	FH1_AGBL5 (CCP5)	CTATATCCAAAGCTCATCTCC	178 bp
RH1_TTLL8	AGTGGAACTTCTTCTCTACC		RH1_AGBL5 (CCP5)	AGTTGCATTCAAGTGTGTAG	
FH1_TTLL9	ATCATGAAGCCTGTAGCC	158 bp	FH1_AGBL4 (CCP6)	AAATGATGATGCCATTGGAG	114 bp
RH1_TTLL9	GGATTTTCAATGTAACGCTG		RH1_AGBL4 (CCP6)	TTACCACTTTCAAAGCAAGC	
FH1_TTLL10	GAAGAGTTTTTCCCAGAGAC	90 bp			
RH1_TTLL10	GATCCATATCTGGGTTTCATC				

Fig. S4. Primers and predicted fragment lengths for qRT-PCR screen of TTLL and CCP expression. Exon overlapping primers were disgned for a qRT-PCR screen of TTLL and CCP expression. Forward and reverse primer sequences are listed, along with predicted fragment length.

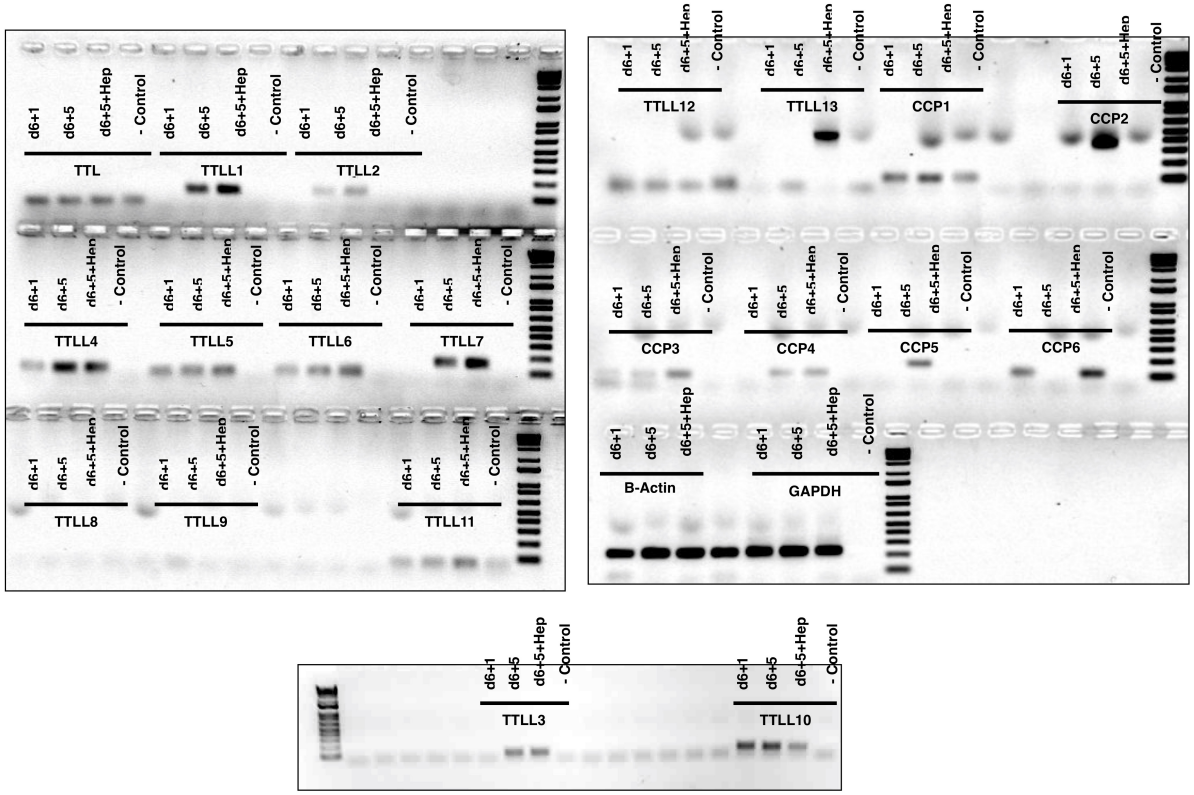

Fig. S5. Whole gel for TTLL10 and CCP RT-PCR screen in iPSC-MKs. Complete gels used in figure 6.

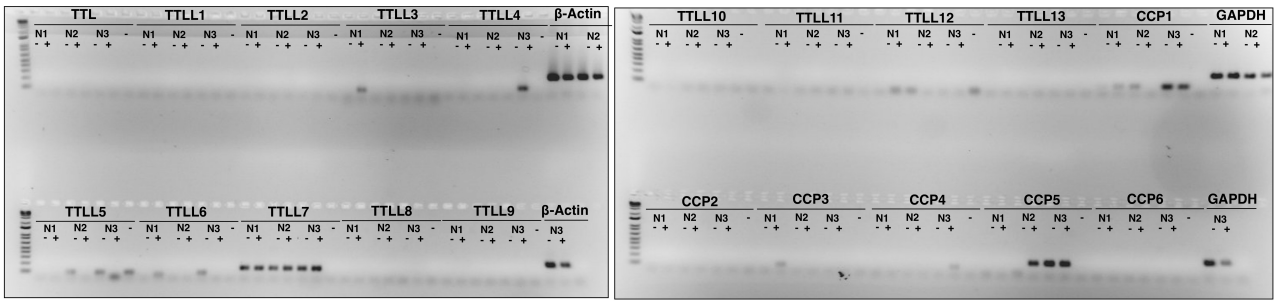

Fig. S6. Whole gel for TTLL10 and CCP RT-PCR screen in human peripheral blood platelets. Complete platelet gel used in figure 6.